PNAS

RESEARCH ARTICLE

Supporting Information for

Impact of Repeated Blast Exposure on Active-Duty United States Special Operations Forces

Natalie Gilmore*, Chieh-En J. Tseng*, Chiara Maffei*, Samantha L. Tromly, Katryna B. Deary, Isabella R. McKinney, Jessica N. Kelemen, Brian C. Healy, Collin G. Hu, Gabriel Ramos Llorden, Maryam Masood, Ryan J. Cali, Jennifer Guo, Heather G. Belanger, Eveline F. Yao, Timothy Baxter, Bruce Fischl, Andrea S. Foulkes, Jonathan R. Polimeni, Bruce R. Rosen, Daniel P. Perl, Jacob M. Hooker, Nicole R. Zürcher, Susie Y. Huang, W. Taylor Kimberly, Douglas N. Greve, Christine L. Mac Donald, Kristen Dams-O'Connor, Yelena G. Bodien**, Brian L. Edlow MD**

* co-first authors
** co-senior authors

Correspondence:
Brian L. Edlow MD
bedlow@mgh.harvard.edu.

This PDF file includes:
Supporting text
Figures S1 to S4
Tables S1 to S24
SI References

Supporting Text.

Screening, Enrollment, and Study Procedures. Of 182 active-duty Special Operations Forces (SOF) personnel who replied to the study advertisement, we screened 87 and enrolled participants until the target of n=30 was met. See Figure S1 for CONSORT diagram.

Validity Assessment for Cognitive Performance and Self-Reported Symptom Measures. We applied standard cutoffs (i.e., > 85% on the Immediate Recall, Delayed Recall, and Consistency scores of the Medical Symptom Validity Test [MSVT] (1); < 8 on the Mild Brain Injury Atypical Symptoms [mBIAS] (2); < 23 on the Validity-10 [a metric derived from the mBIAS]) to assess validity of cognitive performance and self-reported symptom assessment data, respectively. Additionally, we examined the effort and performance validity metrics embedded in the Automated Neuropsychological Assessment Metrics (ANAM) (3) and Philips IntelliSpace Cognition (4) batteries.

7 Tesla MRI Data Acquisition and Processing. Functional MRI data were acquired using an ultra-high spatial and temporal resolution blood-oxygenation level dependent (BOLD) sequence on a 7T scanner, as previously described (5). We used the Terra 7T platform (Siemens Healthineers, Erlangen, Germany) with the vendor-supplied 32-channel head-only receive coil array and birdcage transmit coil (Nova Medical, Wilmington, MA). Notable BOLD sequence parameters include: whole-brain single-shot simultaneous multi-slice (6) gradient-echo echo-planar imaging at 1.2 mm isotropic voxel size, with TR=2.25 sec and multiband factor 3.

We acquired four runs of resting-state fMRI (rs-fMRI), each with 150 measurements. Before the first run and between runs, the participants are asked to remain awake with their eyes open, and to not think about anything specific. We also acquired T_1-weighted data to provide an anatomical reference for the rs-fMRI data, as well as standard calibration and auxiliary data such as magnetic field maps (B_0 and B_1^+) that are used to adjust the system and remove artifacts.

BOLD data were processed in the FreeSurfer 7.3.0 Functional Analysis Stream (FSFAST) (7) for B_0 distortion correction, motion correction, slice-timing correction, and temporal detrending (high-pass filtering at 0.01 Hz and removal of global waveform, ventricular mean waveform, white matter mean

waveform, and motion correction waveforms). Functional networks were identified using Raichle atlas network nodes as seed regions (Figure S2) (8). The anatomic coordinates of network nodes (8) were projected onto the surface of the cerebral cortex as discs with 10mm radius (allowing the mean waveform to be computed exclusively in cortical gray matter), or onto subcortical structures as spheres with a 10mm radius. Brain network functional connectivity was measured as the mean Pearson correlation coefficient between the average BOLD signal within each network's nodes.

Connectome Diffusion MRI Acquisition and Processing. Diffusion MRI (dMRI) data were acquired on a 3 Tesla Connectome scanner (MAGNETOM CONNECTOM Siemens Healthineers, Erlangen, Germany) using a 64-channel custom-made head coil and a two-dimensional (2D) diffusion-weighted pulsed gradient spin echo planar imaging (DW-PGSE-EPI) sequence. We used a previously reported protocol (9) with the following parameters: 2 mm isotropic voxels; TE/TR=77/3800 ms; eight linearly spaced gradient strengths in the range G = 30-290 mT/m per diffusion time; two diffusion times $\Delta = 19$ and $49\,ms;\ \delta = 8\,ms;$ 16 b-values ranging from 50 to 17,800 s/mm^2 with either 32 diffusion-encoding directions (for shells with b ≤ 2,300 s/mm^2) or 64 directions (for shells with b ≥ 2400 s/mm^2); one interspersed b=0 image volume for every 16 diffusion-weighted volumes; GRAPPA acceleration factor R=2. The total acquisition time was 55 minutes. Five volumes without diffusion weighting were also acquired with reversed phase encoding direction to correct for susceptibility-induced distortions. Data were first corrected for gradient nonlinearity distortions (10) using in-house code written in Matlab. Subsequently, we corrected for susceptibility-induced distortion, head motion (both between-volume and within-volume), and eddy-current induced artifacts using the topup and eddy frameworks in FSL 6.0.4 (11-13).

The tensor and the ball-and-stick models were fit to the b≤ 3000 s/mm^2 data using DTIFIT and BEDPOSTX in FSL 6.0.4 (14), and diffusion scalar maps were obtained for each subject. Reconstruction of selected white matter pathways was performed automatically using the global probabilistic tractography algorithm TRACULA in FreeSurfer 7.3.0 (15, 16). Based on previous literature (Table S8), the following 17 pathways were reconstructed in TRACULA: the anterior thalamic radiation (ATR); the dorsal and ventral portions of the cingulum bundle (CBD, CBV); the cortico-spinal tract (CST); the extreme capsule (EmC); the inferior longitudinal fasciculus (ILF); the middle cerebellar peduncle (MCP); the most ventral portion of

the superior longitudinal fasciculus (SLF3); the uncinate fasciculus (UF); the prefrontal, premotor, parietal, temporal, and central portions of the corpus callosum, along with the genu, splenium and rostrum (Figure S3). For each reconstructed pathway the weighted average of fractional anisotropy (FA) across all voxels within each pathway was computed. Before extracting FA, the posterior probability distribution of the pathway estimated by TRACULA was thresholded by masking out all values below 20% of the maximum (15, 16).

T1-Weighted MRI Acquisition and Processing. T1-weighted structural MRI data were acquired on a 3 Tesla Connectome scanner (MAGNETOM CONNECTOM Siemens Healthineers, Erlangen, Germany) using a 64-channel custom-made head coil and a three-dimensional (3D) T_1-weighted multiecho magnetization-prepared rapid gradient echo (MEMPRAGE) sequence (17). Parameters included: 1 mm isotropic resolution, TR/TE = 2530/1.15, 3.03, 4.89, 6.75 ms, GRAPPA acceleration factor R = 2; TI = 1100 ms. We repeated the same protocol twice, and we used both sets of images in the "recon-all" FreeSurfer pipeline. This pipeline performed cortical surface extraction (18), segmentation of subcortical structures, and parcellation of cortical regions (19, 20) based on the Desikan-Killiany atlas. Additionally, we extracted local estimates of cortical thickness for selected regions (Table S11).

[^{11}C]PBR28 TSPO and [^{18}F]MK6240 TAU PET-MRI Acquisition and Processing.

PET-MRI Data Acquisition. Participants were scanned with [^{11}C]PBR28 and [^{18}F]MK6240 PET on separate days. [^{11}C]PBR28 or [^{18}F]MK6240 was administered as a slow bolus injection through an intravenous catheter by a licensed nuclear medicine technologist outside of the scanner. A circularly polarized transmit and an 8-channel MR head receiver coil were used. A high-resolution T1-weighted structural scan was acquired using MEMPRAGE with prospective motion correction (using EPI-based volumetric navigators, vNavs), with TR=2530ms, TE[1-4]=1.66ms, 3.53ms, 5.4ms, 7.27ms, FOV=280mm, flip angle=7deg, voxel size=1mm isotropic (21). Approximately one hour of simultaneous PET-MRI was conducted for each scan and PET data was stored in list-mode format.

Radiotracer synthesis. [^{11}C]PBR28 was synthesized in the MGH Athinoula A. Martinos Center for

Biomedical Imaging Radiotracer Production Lab, as previously described (22). [^{18}F]MK6240 was synthesized at the MGH Gordon Center for Medical Imaging or PETNET Solutions New York.

TSPO genotyping. A venous blood sample was drawn to perform genotyping for the Ala147Thr polymorphism in the TSPO gene. Individuals with the T/T genotype, which confers low binding affinity and negligible PET signal (23), were excluded from the analysis.

PET reconstruction. A validated MR-based methodology with Statistical Parametric Mapping (SPM)–based, pseudo–computed tomography methodology was used for attenuation correction (24, 25). PET data were reconstructed from prompt coincidences using the three-dimensional ordinary Poisson ordered-subset expectation maximization (3D OP-OSEM) algorithm with 32 subsets and 1 iteration, corrected for normalization, isotope decay, dead time, photon attenuation, and random and scatter coincidences. Images were reconstructed into a 256 x 256 x 153 matrix with isotropic voxel dimensions of 1.25 mm.

Pseudo-reference region. The [^{11}C]PBR28 SUV and the [^{18}F]MK6240 SUV in the respective pseudo-reference region (i.e. whole brain without ventricles for [^{11}C]PBR28 PET and isthmus cingulate cortex for [^{18}F]MK6240 PET) were not significantly different between blast exposure groups (Table S23).

Region of interest (ROI) mask generation. Selected ROIs were determined based on previous literature for TSPO (Table S9) and Tau (Table S10). *TSPO.* ROI masks were generated from each individual's FreeSurfer parcellations by combining the gray and white matter parcellations. The gray-white matter junction ROI mask was generated by projecting from 25% of the thickness inside the white matter to 25% of the thickness inside the cortex for each subject. The gray-white matter junction was selected as ROI based on postmortem findings of astroglial scarring at the gray-white matter junction in blast-exposed military service members (26, 27). *Tau.* Cortical and cerebellar cortex ROI masks were generated from each individual's FreeSurfer parcellations and segmentations. The cerebellar cortex ROI masks were eroded by 2mm from the outer edge to account for the potential spill in due to off-target binding of [^{18}F]MK6240 in nearby extra-cerebral regions.

Data Quality Assessments.

Cognitive performance, psychological health, and physical symptom data quality assessments. Data entry and scoring were checked for 20% of the sample who participated in the study (i.e., for every six participants to ensure random selection of datapoints to check). To further reduce potential for bias in the process, data quality assessment for these measures was performed by a member of the study team that was not involved in the data acquisition, scoring, and entry during the study visit. The independent data monitor checked the scoring accuracy for all source data, whether stored on paper form or REDCap (28) (a HIPPA-compliant web-based application used for electronic study data acquisition and storage). Any discrepancies in scoring or data entry were documented in a log by the data monitor. The study team member initially responsible for assessment, data scoring, and entry was notified of any discrepancies. Those mistakes were corrected on the paper form and in REDCap. The data monitor then checked that the changes had been made accurately. All discrepancies and subsequent corrections were documented by both the monitor and original assessor. Data quality was also assessed by group of team members with expertise in neuropsychological and neurobehavioral assessment that were not involved in the acquisition, scoring, or study data entry by inspecting the distribution of each measure (e.g., ensure no outliers, implausible data points based on the measures range, missing data).

Blood proteomics data quality assessment. For blood biomarker data, analytes were measured using the Neuro 3-plex, Neuro 4-plex, and p-Tau181 V2 assays (Quanterix). Each target protein had an average coefficient of variation <5% among all experimental samples within the linear range of the assay, with the exception of UCHL1, which was excluded from analysis because n=5 (16%) of samples were within the linear range, n=14 (47%) were below the lower limit of quantification, and n=11 (37%) were below the limit of detection.

Neuroimaging data quality assessment overview. All subjects were processed using fully automated pipelines to minimize processing errors. The quality of neuroimaging data was assessed through visual inspection by multiple members of the study team before and after pre-processing. We extracted automated measures of signal-to-noise ratio and head motion for further assessment of data quality. All MRI and PET-

MRI data across scanners and modalities were first pre-processed and then co-registered to the individual T1-weighted images of each subject to facilitate visual inspection. The imaging team screened each dataset for acquisition artifacts, noise, or processing errors.

Resting-state functional MRI data quality assessment. The resting-state fMRI scans for two subjects were removed from analysis due to severe signal dropouts that could not be corrected.

Diffusion MRI data quality assessment. Automated quality control quantitative reports were produced for each subject. The reports included volume-to-volume motion, within volume motion, outliers, and signal-to-noise ratio. Data were also stored in a format convenient for group analysis. The relative and absolute volume-to-volume motion were similar to previously reported ranges (0.52 +/- 0.07 mm and 2.38 +/- 0.70 mm, respectively) (29), and no subject was excluded due to severe overall head motion. One subject had severe head rotations for some of the acquired diffusion-weighted volumes that were not successfully corrected during preprocessing in FSL. For this subject, we computed the rigid transform between the rotated b=0 volume and the unrotated closest b=0 volume using mri_coreg in FreeSurfer 7.3.0 and applied the transformation to the corresponding diffusion-weighted volumes. We applied the same rotation to the diffusion gradient directions. The average SNR within the whole brain was 15.5 +/- 2.29 for b < 100 s/mm^2 volumes. The automated reconstructions of white matter pathways obtained in TRACULA were visually assessed for each subject by C.M. to ensure anatomical accuracy of the reconstructions.

PET-MRI data quality assessment. The MRI-based attenuation map used for PET data reconstruction was visually inspected by C.J.T. to ensure that it followed the participant's head anatomy. The T1-weighted structural image for 3 subjects required denoising to generate an anatomically correct attenuation map. The reconstructed SUV was visually inspected for artifacts generated by dead blocks. If any artifacts were noticed, the dead blocks detected were excluded in the reconstruction to eliminate the artifacts. Motion was estimated using the realignment matrices derived from the motion correction step of the five-minute SUV frames. The PET data motion estimates of all participants were within 3mm (approximately the spatial

resolution of the BrainPET) and considered minimal. Additionally, the SUV was visually inspected to identify known characteristics of [^{11}C]PBR28 and [^{18}F]MK6240 images.

Cortical thickness data quality assessment. For T1-weighted images, results of the "recon-all" FreeSurfer pipeline were visually inspected for each subject for skull strip errors, segmentation errors, and pial surface misplacement, and erroneous labeling (i.e., using the Desikan-Killiany atlas (30) parcellation as shown in Figure S4) was manually corrected by D.N.G.

Complementary Statistical Analysis. After dividing the cohort into two groups of 15 participants based on a median split of the GBEV, we performed t-tests comparing the GBEV above median group ($GBEV_a$) to the GBEV below median group ($GBEV_b$) on each measure, in addition to the linear regression analyses reported in the main manuscript. These results are shown in Tables S12-S19. Demographic and exposure results for the $GBEV_a$ and the $GBEV_b$ groups are provided in Table S24.

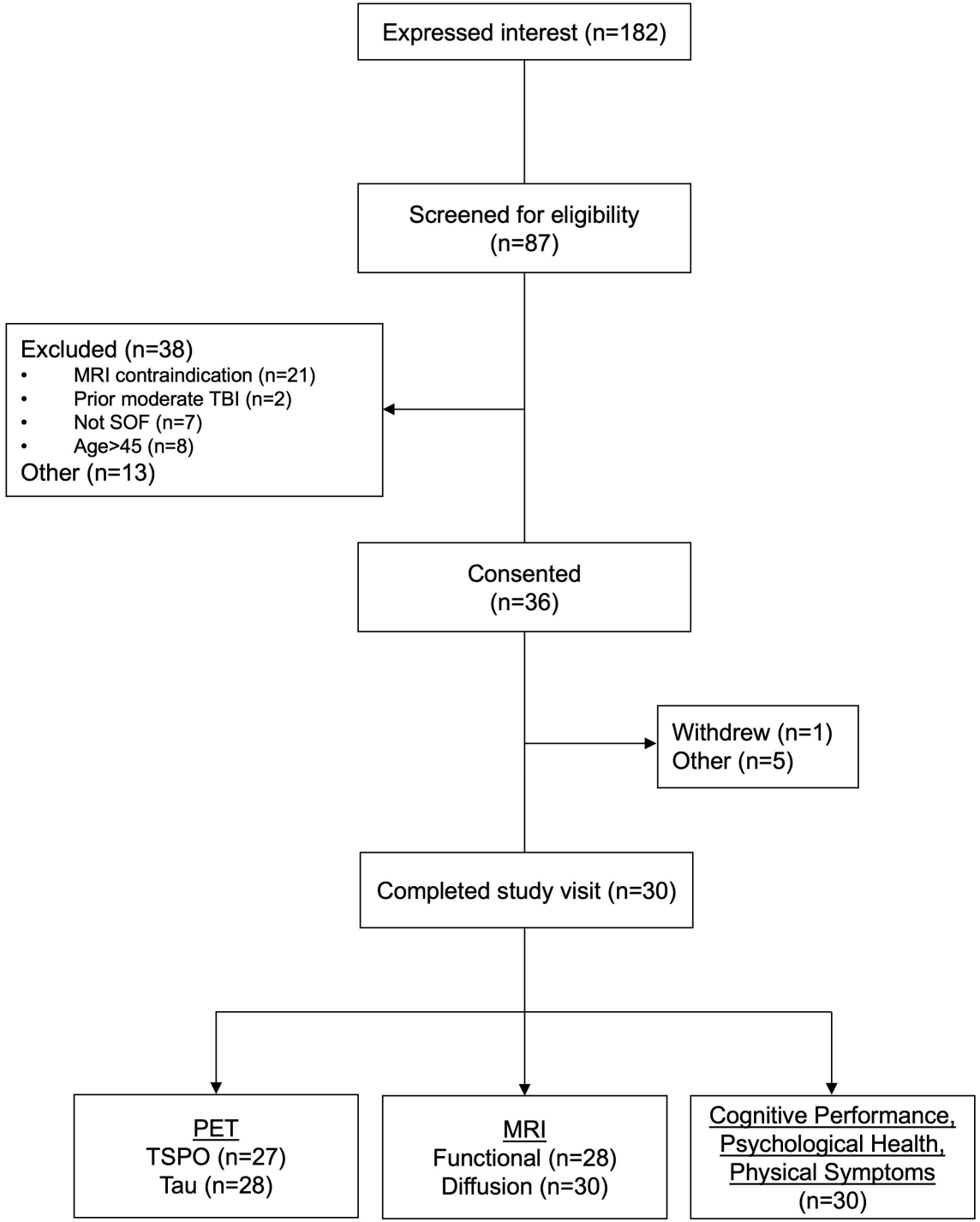

Figure S1. Screening and Enrollment of Study Subjects.
A recruitment flyer was sent via email by United States Special Operations Command (USSOCOM) to Special Operations Forces (SOF) units in the Army, Navy, Air Force, and Marines. We were contacted by 182 individuals, of whom we screened 87 to reach the enrollment target of 30. The most common exclusion criterion was an MRI contraindication (e.g., metallic shrapnel). Of 36 consented participants, 1 withdrew and 5 were unavailable to travel to the study site due to training and deployment schedules. All 30 consented participants completed the assessments of cognitive performance, psychological symptoms, physical health, blood proteomics, and 3 Tesla Connectome MRI. Three participants had an Ala147Thr polymorphism in the translocator protein (TSPO) gene that confers low affinity binding and thus, their data could not be included in the TSPO positron emission tomography (PET) analysis. Two Tau PET scans could not be completed due to PET radiotracer production failure. Two 7 Tesla resting-state functional MRI scans were acquired but not included in data analysis due to signal inhomogeneities.

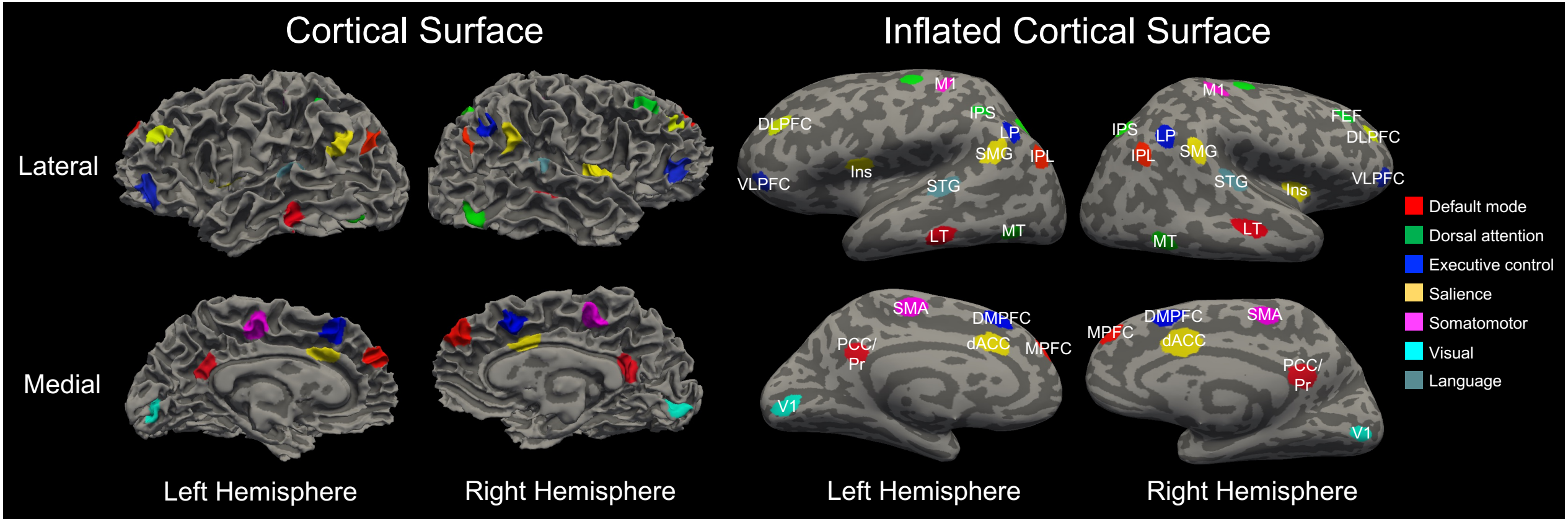

Figure S2. Network Nodes for Resting-state MRI Functional Connectivity Analysis.
Seven functional brain networks were identified using nodes from the Raichle network atlas (Raichle. *Brain Connectivity* 2011). Nodes are shown on the lateral (top row) and medial (bottom row) surface of the cortex (left) and on the inflated cortical surface (right) for one representative participant. The anatomic location of network nodes is labeled on the inflated cortical surface.

Abbreviations: dACC = dorsal anterior cingulate cortex; DLPFC = dorsolateral prefrontal cortex; DMPFC = dorsomedial prefrontal cortex; FEF = frontal eye fields; IPL = inferior parietal lobule; IPS = intraparietal sulcus; LP = lateral parietal; LT = lateral temporal lobe; M1 = primary motor cortex; MT = middle temporal region; PCC/Pr = posterior cingulate cortex/precuneus; SMA = supplementary motor area; SMG = supramarginal gyrus; STG = superior temporal gyrus; Ins = insula; V1 = visual cortex; VLPFC = ventrolateral prefrontal cortex.

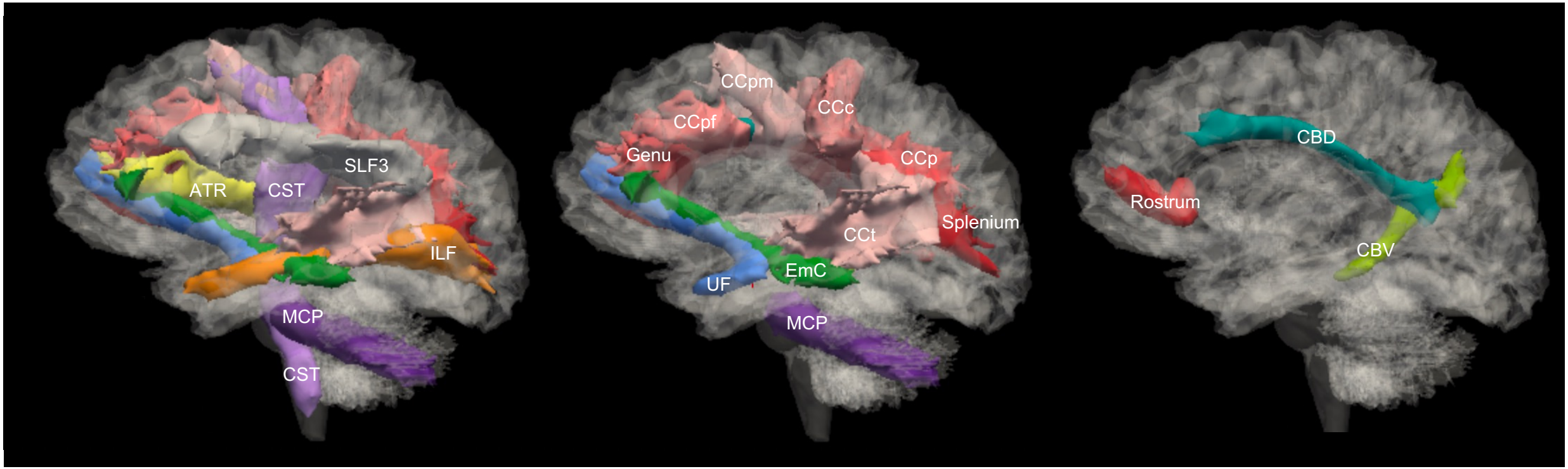

Figure S3. White Matter Regions for Diffusion MRI Analysis.
3D reconstruction for a representative participant of the 17 white matter pathways selected for analysis. Three sagittal views (from lateral [left] to medial [right]) are shown, overlaid onto a 3D semitransparent mesh.

Abbreviations: ATR = anterior thalamic radiation; CBD = cingulum bundle dorsal; CBV = cingulum bundle ventral; CCpf = pre-frontal section of the corpus callosum; CCp = parietal section of the corpus callosum; CCpm = pre-motor section of the corpus callosum; CCc = central section of the corpus callosum; CCt = temporal section of the corpus callosum; CST = corticospinal tract; EmC = extreme capsule; ILF = inferior longitudinal fasciculus; MCP = middle cerebellar peduncle; SLF3 = superior longitudinal fasciculus 3; UF = uncinate fasciculus.

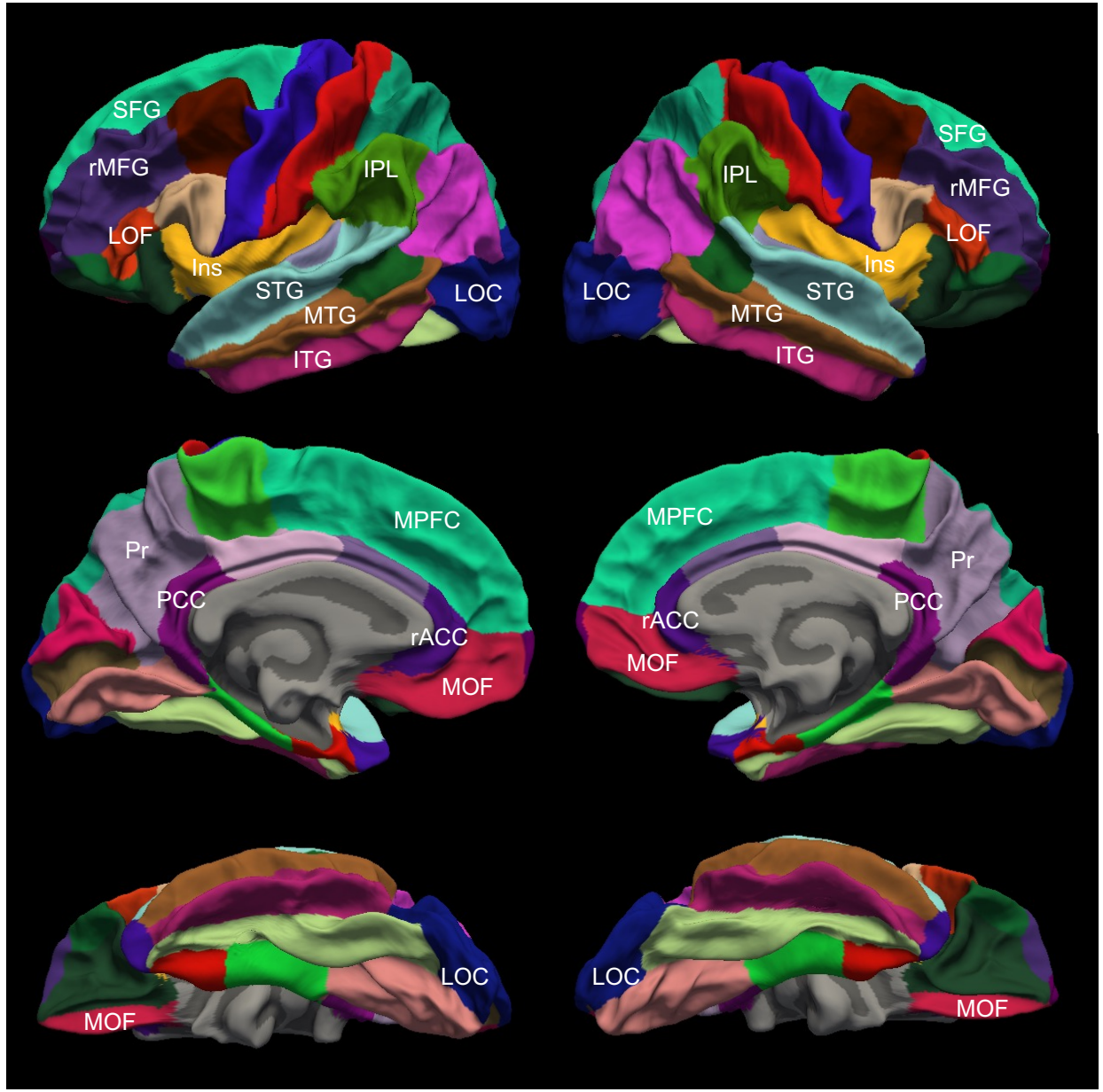

Figure S4. Regions of Interest for Cortical Thickness, TSPO PET-MRI, and Tau PET-MRI Analyses.
The lateral (top row), medial (middle row) and inferior (bottom row) surfaces of the brain are shown for a representative subject. The cerebral cortex is parcellated and color-coded according to the Desikan-Killiany atlas (Desikan et al. *NeuroImage* 2006) using FreeSurfer 7.3.0 (Fischl et al. *NeuroImage* 1999). Anatomic labels are provided for the cortical regions that were selected for analysis based on prior literature (Supplementary Tables 9, 10, and 11).

Abbreviations: Ins = insula; IPL = inferior parietal lobule; ITG = inferior temporal gyrus; LOC = lateral occipital cortex; LOF = lateral orbitofrontal cortex; rMFG = rostral middle frontal gyrus; MOF = medial orbitofrontal cortex; MPFC = medial prefrontal cortex; MTG = middle temporal gyrus; PCC = posterior cingulate cortex; Pr = precuneus; rACC = rostral anterior cingulate cortex; SFG = superior frontal gyrus; STG = superior temporal gyrus.

Table S1. Inclusion and Exclusion Criteria

Inclusion
25-45 years of age
Male[a]
Active-duty SOF
History of combat deployment confirmed by VA or DoD records[b]
History of combat exposure during any deployment verified by the CES[c]
Exclusion
History of moderate or severe TBI[d]
History of major neurologic disorder
Untreated or unstable severe psychiatric condition
Current severe medical condition that requires long-term treatment
Imaging contraindications[e] including safety concerns, medical conditions that could affect cerebral metabolism, or use of certain medications
Any condition that may cause undue risk to the subject or create a logistical or safety contraindication to enrollment

Abbreviations: CES = Combat Exposure Scale; DoD = Department of Defense; MRI = magnetic resonance imaging, PET = Positron Emission Tomography; SOF = Special Operations Forces; TBI = traumatic brain injury; VA = Veterans Affairs.

[a] We excluded females because the majority of SOF who are exposed to repeated blasts are male. Including females could have resulted in an imbalance across the blast exposure groups.

[b] Deployed to a region of conflict while serving in the U.S. military.

[c] The CES measures the degree of combat exposure. Endorsement of any item on the CES ensured that all participants experienced combat during their military career.

[d] We administered the Brain Injury Screening Questionnaire (BISQ) and used the VA/DoD definition of moderate/severe TBI: initial Glasgow Coma Scale score < 13, coma duration > ½ hour, post-traumatic amnesia duration > 24 hour, or abnormal structural brain imaging, to identify individuals with a history of moderate or severe TBI.

[e] An MRI safety team was convened to collect and review all medical records pertaining to prior surgeries or exposures to implanted metal. MRI contraindications included any metal in the body that would make an MRI scan unsafe (most commonly shrapnel or a metal implant for which no MRI safety information could be obtained), pre-existing medical conditions including a likelihood of developing seizures or claustrophobic reactions, inability to lie supine for up to 2 hours in the MRI scanner, and > 300 pounds due to the MRI table's weight limit. Prior radiation exposure of ≥ 50 mSv over the past 12 months was a contraindication for PET imaging.

Table adapted from Edlow, Bodien et al. *Journal of Neurotrauma*, 2022 (31).

Table S2. Overview of Study Procedures

Measure	Study Activity	Screening	Pre-Visit	2-day study visit
Blast & Combat Exposure	GBEV, CES	X		
TBI History	BISQ	X		
Imaging Safety	MRI/PET Contraindications	X		
Self-Report Measures of Psychological Health and Physical Symptoms	*Electronic Survey:* MOS, DVBIC, DRRI, BPAQ, PSQI, PCL-5, TBI-QOL short-forms, AUDIT-C, PROMIS Pain Interference and Intensity, HIT-6, WHODAS 2.0, DAST-10		X	
	In-person Interview: STOP-BANG, PHQ-9, GOSE, FrSBE (self and family), SBQ-R, BGLHA, NSI, mBIAS, MSVT, NIH TBI CDE: Medical History			X
Cognitive Performance Measures	*Standard Neurocognitive Tests:* ANAM, WAIS-IV Arithmetic/Digit Span, MSVT, TOPF, Grooved Pegboard, DKEFS Color-Word Interference, ACT, Pupillometry Test			X
	Philips IntelliSpace Cognition iPad-based Tests[a]*:* RAVLT, Trail Making, Letter Fluency, Star Cancellation, Clock Drawing/Copy, Rey-Osterrieth Complex Figure, Category Fluency, and Digit Span			X
Neuroimaging	Connectome MRI			X
	7 Tesla MRI			X
	TSPO PET-MRI			X
	Tau PET-MRI			X
Blood Proteomics	Blood Draw			X

[a] Philips IntelliSpace Cognition iPad-based tests are based on widely used analog neuropsychological assessments, with slight modifications to administration procedures and scoring criteria.

Abbreviations: ACT= Auditory Consonant Trigrams; ANAM = Automated Neuropsychological Assessment Metrics; AUDIT-C = Alcohol Use Disorders Test-Consumption; BISQ = Brain Injury Screening Questionnaire; BGLHA = Brown-Goodwin Assessment for Lifetime History of Aggression; BPAQ = Buss-Perry Aggression Questionnaire; CES = Combat Exposure Scale; DAST-10 = Drug Abuse Screening Test; DVBIC = Defense and Veterans Brain Injury Center; DKEFS= Delis-Kaplan Executive Function System; DRRI = Deployment Risk and Resilience Inventory Combat Experiences Scale, modified for STRONG STAR; FrSBE = Frontal Systems Behavior Scale; GBEV = Generalized Blast Exposure Value; GOSE = Glasgow Outcome Scale – Extended; HIT-6 = Headache Impact Test; mBIAS = mild Brain Injury Atypical Symptoms; MOS = Military Occupational Specialty; MRI = Magnetic Resonance Imaging; MSVT= Medical Symptom Validity Test; NIH TBI CDE = National Institutes of Health, Traumatic Brain Injury, Common Data Elements; NSI= Neurobehavioral Symptom Inventory; PCL-5 = The PTSD Checklist for DSM-5; PET = Positron Emission Tomography; PHQ-9 = Patient Health Questionnaire-9; PROMIS = Patient-Reported Outcomes Measurement Information System; PSQI = Pittsburgh Sleep Quality Index; RAVLT= Rey Auditory Verbal Learning Test; SBQ-R = Suicide Behaviors Questionnaire-Revised; STOP-BANG= Snoring history, Tired during the day, Observed stop breathing while sleep, high blood Pressure, BMI more than 35 kg/m2, Age more than 50 years, Neck circumference more than 40 cm and male Gender; TBI-QOL = TBI Quality of Life; TSPO = Translocator protein; WAIS-IV = Wechsler Adult Intelligence Scale, 4th edition; TOPF = Test of Premorbid Functioning; WHODAS 2.0 = World Health Organization Disability Assessment Schedule 2.0.

Table adapted from Edlow, Bodien et al. *Journal of Neurotrauma*, 2022.

Table S3. Demographics, Exposures, Cognitive Performance, Psychological Health, and Physical Symptom Assessments

Measure	Construct Measured/ Data Collected	Administration Method
Demographics	Age, ethnicity, race, education	REDCap survey pre-visit
Military History	Military history, rank, time in service (years)	
Military occupational status	Blast exposure (indirect)	
Generalized Blast Exposure Value	Blast exposure	Pre-visit by phone
Deployment Risk & Resiliency Inventory, Combat Experiences Scale, modified for STRONG STAR*	Combat exposure	REDCap survey pre-visit
Medical History	Symptom characteristics, duration, severity, and treatment	In-person visit - interview
Brain Injury Screening Questionnaire	Lifetime TBI exposure	Pre-visit by phone; follow-up in-person
Pittsburgh Sleep Quality Index	Sleep quality & disturbances	REDCap survey pre-visit; spouse by-phone
STOP BANG	Obstructive sleep apnea	In-person visit
Pupillometry Exam	Pupil constriction and dilation	
Automated Neuropsychological Assessment Metrics	Processing speed, memory, inhibition, and other cognitive processes	In-person, laptop
Philips IntelliSpace Cognition	Memory, processing speed, language, executive function, visuospatial function	In-person visit, iPad
Grooved Pegboard Test	Fine motor function	In-person visit
Delis-Kaplan Executive Function System	Inhibitory control, cognitive flexibility	
WAIS- Wechsler Adult Intelligence Scale, 4th version, Digit Span and Arithmetic	Working memory	
Test of Premorbid Functioning	Premorbid ability/cognitive reserve	
Auditory Consonant Trigrams	Divided attention, working memory	
Patient Health Questionnaire-9	Depression	In-person visit
Suicidal Behaviors Questionnaire-Revised	Suicidality	
Neurobehavioral Symptom Inventory	Post-concussive symptoms	
Brown-Goodwin Lifetime History of Aggression	Aggression	

Measure	Construct Measured/ Data Collected	In-person visit
Glasgow Outcome Scale - Extended	Global outcome	
Mild Brain Injury Atypical Symptoms	Symptom validity/effort	
Medical Symptom Validity Test	Symptom validity/effort	
Frontal Systems Behavior Scale	Apathy, disinhibition, executive dysfunction	Participant: In-person visit
		Spouse: by phone
PTSD Checklist for DSM-5	Post-traumatic stress disorder	REDCap survey pre-visit
RAND-36 Health-Related Quality of Life	Physical functioning, role limitations, energy/fatigue, emotional well-being, social functioning, pain, general health	
TBI-Quality of Life short forms	Anger	
	Anxiety	
	Emotional & behavioral dyscontrol	
	Resilience	
Buss-Perry Aggression Questionnaire	Aggression	
World Health Organization Disability Assessment Schedule 2.0	Cognition, mobility, self-care, getting along, life activities, participation	
Alcohol Use Disorders Identification Test	Alcohol screening	
Drug Abuse Screening Test	Drug screening	
Headache Impact Test-6	Headaches	
PROMIS Short forms	Pain Intensity	
	Pain Interference	

Abbreviations: STOP-BANG = Snoring history, Tired during the day, Observed stop breathing while sleep, High blood pressure, BMI more than 35 kg/m^2, Age more than 50 years, Neck circumference more than 40 cm and male Gender; PTSD = Post-traumatic Stress Disorder; DSM = Diagnostic and Statistical Manual of Mental Disorders; WHO = World Health Organization, PROMIS = Patient-Reported Outcomes Measurement Information System; REDCap = Research Electronic Data Capture. Table adapted from Edlow, Bodien et al. *Journal of Neurotrauma*, 2022 (31).

Table S4. Selection of Variables for Cognitive Performance Testing

Assessment	Measure	Author	Journal	Year	Finding
ANAM	SRT Throughput	Haran et al.	*Applied Neuropsychology: Adult*	2019	N=27 blast-exposed veterans had decreased performance compared to n=36 non-blast exposed veterans
	SR2 Throughput				
	SR2 Mean RT (ms)	Tate et al.	*Journal of Neurotrauma*	2013	N=21 NZDF had slower RT after blast exposure
	CDS (% correct)				N=5 NZDF participants with highest ANAM composite scores had slower response times than N=5 participants with lowest composite scores
	MTS mean RT (ms)				NZDF slower after blast exposure compared to baseline
	CDD (% correct)				NZDF had fewer correct responses on CDD after day 2 compared to baseline
	M2S (% correct)				NZDF had slower RT after day 2 exposure compared to baseline
Philips TMT	A duration (secs)	Rhea et al.	*Military Medicine*	2017	N=29/59 active-duty participants showed cognitive decline following blast exposure
	B duration (secs)				
Philips RAVLT	Learning Trials Total				
	Delayed Recall total				

Abbreviations: ANAM = Automated Neuropsychological Assessment Metrics; SRT = Simple Reaction Time; SR2 = Simple Reaction Time Repeat; New Zealand Defense Forces = NZDF; CDS = Code Substitution — Learning; Code Substitution — Delayed; M2S = Matching to Sample; MTS = Mathematical Processing; TMT = Trail Making Test; RAVLT = Rey Auditory Verbal Learning Test

Table S5. Selection of Variables for Self-Report Assessments of Psychological Health and Physical Symptoms

Assessment	Measure	Author	Journal	Year	Finding
Neurobehavioral Symptom Inventory	Total Score	Petrie et al.	*Journal of Neurotrauma*	2014	N=34 blast-exposed veterans had higher NSI scores compared to n=18 control veterans
		Reid et al.			N=505 active-duty participants had higher NSI scores compared to n=68 non-blast exposed active-duty participants as blast increased
Rivermead Post-Concussive Questionnaire		Vartanian et al.	*Journal of Military, Veteran and Family Health*	2022	N=62 active-duty participants had higher early and late concussive symptom scores compared to n=28 controls
			Military Medicine	2021	N=70 active-duty breachers endorsed higher late concussive symptoms after year 4 compared to n=14 controls
			Frontiers in Neurology	2020	N=19 breachers and range staff scored higher on early and late concussive symptom questionnaire than n=19 controls
Interpersonal Measure of Psychopathy*		Mendez et al.	*Brain Injury*	2013	N=12 blast-exposed veterans had higher IM-P total scores and aggression scores compared to n=12 non-blast exposed veterans
Headache Impact Test-6		MacDonald et al.	*Brain*	2015	N=38 active-duty participants with blast TBI exposure had significantly higher HIT-6 scores compared to n=34 controls
		Woodall et al.	*Military Medicine*	2021	N=10/11 active-duty mortarmen endorsed headaches following 3 days of blast-exposed training compared to N=1/4 controls
		Tate et al.	*Journal of Neurotrauma*	2013	N=5 NZDF participants with highest ANAM composite scores reported more frequent and severe headaches than N=5 participants with lowest ANAM composite scores
RAND-36	Physical Functioning	Vartanian et al.	*Military Medicine*	2021	N=70 active-duty breachers scored lower than n=14 controls on all RAND-36 subscales
	Role limitations due to physical health				
	Energy and fatigue		*Frontiers in Neurology*	2020	N=19 active-duty breachers scored lower than n=19 on all subscales except social functioning. Both groups scored the same on RAND-36 social functioning subscale
	Social functioning				
	General health				

* Based on the findings of this study using the IM-P (a measure that was not used in the current study), the relationship between the Buss-Perry Aggression Questionnaire and GBEV was tested, as the Buss-Perry Aggression Questionnaire was the closest measure to that used by Mendez et al.

Table S6. Selection of Variables for Blood Proteomics

Measure	Author	Journal	Year	Finding
Neurofilament Light (NfL)	Vorn et al.	*Frontiers: Neuroscience*	2022	N=34 active-duty participants had increased serum concentration of NfL, Ptau181 and serum tau from day 1 to day 7 blast exposure
Phosphorylated Tau181 (Ptau181)				
Tau				
Ubiquitin carboxyl-terminal esterase L1 (UCH-L1)	Boutté et al.	*JAMA Network Open*	2021	N=106 active-duty participants had higher serum levels of UCH-L1, AB40, and AB42 compared to n=30 civilian controls
Amyloid Beta 40 (AB40)				
Amyloid Beta 42 (AB42)				
NfL	Boutté et al.	*PLOS One*	2019	N=29 active-duty participants in breacher course had elevated serum NfL after one day of exposure
Glial Fibrillary Acidic Protein (GFAP)	Tschiffely et al.	*Journal of Neurotrauma*	2020	N=50 active-duty participants in 10-day breacher training had decreased GFAP concentrations on day 6 and 7. GFAP was negatively correlated with cumulative blast exposure.

Table S7. Selection of Variables for Resting-state Functional MRI

Measure	Author	Journal	Year	Finding
Executive Control Network	Han et al.	*Neuroimage*	2014	N=63 blast-exposed active-duty participants had abnormally low functional connectivity in the executive control network related to controls
Default Mode Network				
Salience Network				
Executive Control Network	Pagulayan et al.	*Brain Imaging and Behavior*	2018	N=24 blast-exposed veterans had increased functional connectivity from the frontal seed regions to cortical and subcortical regions compared to n=17 control veterans
Default Mode Network				
Default Mode Network	Robinson et al.	*Journal of Neurotrauma*	2017	N=116 blast-exposed veterans showed a difference in functional connectivity compared to n=159 control veterans
Somatomotor			2015	
Default Mode Network	Stone et al.	*Journal of Neurotrauma*	2020	N=20 military breachers showed higher internetwork connectivity from DMN to normally anticorrelated task-control network regions compared to n=14 controls
Executive Control Network	Newsome et al.	*Journal of International Neuropsychological Society*	2015	N=17 veteran participants showed altered functional connectivity compared to n=15 veteran controls

Table S8. Selection of Variables for Diffusion MRI

Measure	Author	Journal	Year	Finding
MCP CBD Bundles projecting to orbitofrontal WM (UF, Genu of the CC, Rostrum)	Mac Donald et al.	*New England Journal of Medicine*	2011	N=18/63 military participants had DTI abnormalities (in 2 or more regions); only 2/63 healthy subjects would be expected to have 2 or more abnormalities, emphasizing that the findings in the military sample were not based on chance alone.
MCP CBD CC Bundles projecting to orbitofrontal WM (UF, Genu, Rostrum)	Stone et al.	*Journal of Neurotrauma*	2020	N=20 military and law enforcement breachers had decreased FA compared to n=14 military and law enforcement controls
Genu of the CC (Right hemi only)	Petrie et al.	*Journal of Neurotrauma*	2014	N=34 blast-exposed veterans had lower FA values in the genu of the CC compared to n=18 non-blast exposed veterans
Splenium/Genu of the CC ATR CST	Davenport et al.	*NeuroImage*	2012	N=25 blast-exposed veterans had a greater number of voxels with low FA in 10/20 ROIs compared to n=33 non-blast exposed veterans
Body of the CC CST	Harrington et al.	*Diagnostics (Basel)*	2022	N=20 blast-exposed active-duty participants had abnormally decreased RD, increased FA, and increased axial/radial diffusivity ratio compared to N=19 active-duty controls
ATR CBD	McClelland et al.	*Neuroradiology*	2018	N=16 blast-exposed veterans had higher FA compared to n=18 non-blast exposed veterans
CBV, ATR, SLF3, UF	Yeh et al.	*Human Brain Mapping*	2016	N=202 active-duty participants with blast-exposure showed white matter injury in the fronto-limbic, fronto-striatal, and fronto-parieto-temporal tracts compared to N=50 active-duty controls
Genu of the CC SLF3, ATR, ILF, EmC, CST	Taber et al.	*Journal of Head Trauma Rehabilitation*	2015	N=29 blast-exposed veterans showed significantly lower FA and increased RD compared to n=16 non-blast exposed veterans
CC, CST, CBD	Ivanov et al.	*Frontiers Neurology*	2017	N=16 blast-exposed veterans and N=24 blast-exposed veterans with mild TBI had reduced FA as blast exposure increased

Abbreviations: ATR = anterior thalamic radiation, CBD = cingulum bundle dorsal, CC = corpus callosum, CBV = cingulum bundle ventral, CST = corticospinal tract, EmC = extreme capsule; ILF = inferior longitudinal fasciculus, MCP = middle cerebellar peduncle, SLF3 = superior longitudinal fasciculus 3, UF = uncinate fasciculus.

Table S9. Selection of Variables for [^{11}C]PBR28 translocator protein (TSPO) PET-MRI

Region of Interest	Author	Journal	Year	Finding
Gray-white junction	Shively et al.	*Lancet: Neurology*	2016	N=5 chronically blast-exposed military service members had astroglial scarring at the gray-white junction in several brain regions, including the prefrontal cortex and anterior cingulate cortex
rACC				
mOFC				
SFG				
rMFG				

Abbreviations: mOFC = medial orbitofrontal cortex; rMFG = rostral middle frontal gyrus; rACC = rostral anterior cingulate cortex; SFG = superior frontal gyrus.

Table S10. Selection of Variables for [^{18}F]MK6240 Tau PET-MRI

Measure	Author	Journal	Year	Finding
IFGtri	Robinson et al.	*Neuroimage: Clinical*	2019	N=16 male veterans had higher Tau uptake in the cerebellar, occipital, inferior temporal, and frontal regions, which was correlated with higher blast exposure
MTG				
ITG				
LOC				
Pericalcarine cortex				
rMFG				
IPL				
Cerebellar gray matter				

Abbreviations: IFGtri = pars triangularis of the inferior frontal gyrus; IPL = inferior parietal lobule; ITG = inferior temporal gyrus; LOC = lateral occipital cortex; MTG = middle temporal gyrus; rMFG = rostral middle frontal gyrus.

Table S11. Selection of Variables for T1-weighted Cortical Thickness

Measure	Author	Journal	Year	Finding
Right SFG	Vartanian et al.	*Military Medicine*	2021	N=70 male breachers had lower baseline gray matter volume compared to n=14 non-breacher controls
Occipital lobe ROIs (i.e., cuneus, pericalcarine, lingual gyrus), DMN ROIs (i.e., ITG, MTG, SMG)	Stone et al.	*Journal of Neurotrauma*	2020	N=20 military breachers had increased cortical thickness compared to n=14 military and law enforcement controls
bilateral lOFC, bilateral rMFG, bilateral mOFC, Left SFG, Left rACC, LPFC; Right lFGorb, Right lFGtri, Right insula	Eierud et al.	*NeuroImage: Clinical*	2019	N=41 blast-exposed mild TBI participants had reduced cortical thickness compared to n=41 non blast-exposed mild TBI participants
Left OFC, Left MFG (i.e., rostral and caudal MFG); Right lFG (i.e., triangularis, orbitalis, opercularis)	Clark et al.	*Frontiers: Neurology*	2018	N=51 blast-exposed veterans with mild TBI had greater cortical thinning in frontal regions compared to n=29 blast-exposed veterans without mild TBI
Right ITG, Right insula, Right lFG	Michael et al.	*Journal of Neurotrauma*	2015	N=38 blast-exposed veterans with mild-TBI and n=17 blast-exposed veterans with mod-TBI had cortical thinning in the right inferior temporal, right insula, and right inferior frontal areas compared to n=58 civilian controls
Left STG (banks of superior temporal sulcus), bilateral SFG	Tate et al.	*Brain Imaging Behavior*	2014	N=12 blast-injured, mild TBI participants had significant clusters of cortical thinning compared to N=11 healthy, non-injured recently deployed controls

Abbreviations: DMN = default mode network; IFG = inferior frontal gyrus; lFGorb = pars orbitalis; lFGtri = pars triangularis; ITG = inferior temporal gyrus; lOFC = lateral orbitofrontal cortex; mOFC = medial orbitofrontal cortex; LPFC = lateral prefrontal cortex; MFG = middle frontal gyrus; MTG = middle temporal gyrus; OFC = orbitofrontal cortex; rACC = rostral anterior cingulate cortex; rMFG = rostral MFG; SFG = superior frontal gyrus; STG = superior temporal gyrus; ITG = inferior temporal gyrus; MTG = middle temporal gyrus; SMG = supramarginal gyrus.

Note: Regions that showed a unilateral association with blast exposure in prior literature were tested bilaterally in the current study given only preliminary mechanistic rationale for repeated blast exposure to preferentially affect one hemisphere over another. For example, medial structures in the left hemisphere could be more affected using shoulder-fired weapons that are commonly configured for right-handed operation (i.e, the blast overpressure has greater potential to travel through the left orbit than the right orbit as the latter is protected by the optic).

Table S12. Summary of Associations Between Cognitive Performance Variables and Log-transformed GBEV

Measure	Full Sample M (SD); n	GBEVbelow (b) median group M (SD); n	GBEVabove (a) median group M (SD); n	$GBEV_a$ vs $GBEV_b$ t-statistic, difference in group means, (95% CI); p-value	Unadjusted regression standardized beta, (95% CI); p-value	Adjusted regression standardized beta, (95% CI); p-value Covariates: age, combat exposure, blunt head trauma	Adjusted regression standardized beta, (95% CI); p-value Covariates: age, combat exposure, blunt head trauma, and PTSD symptom severity
ANAM CDD % correct	89.26 (10.86); 30	92.04 (7.19); 15	86.48 (13.28); 15	-1.43, -5.56 (-13.65, 2.54); 0.17	-0.21 (-0.58, 0.17); 0.28	-0.16 (-0.54, 0.22); 0.40	-0.16 (-0.55, 0.23); 0.41
ANAM CDS % correct	97.87 (3.09); 30	97.68 (2.66); 15	98.05 (3.55); 15	0.32, 0.37 (-1.99, 2.73); 0.75	0.11 (-0.27, 0.50); 0.56	0.18 (-0.28, 0.64); 0.42	0.19 (-0.28, 0.66); 0.41
ANAM M2S % correct	97.00 (5.35); 30	96.33 (6.94); 15	97.67 (3.20); 15	0.68, 1.34 (-2.78, 5.45); 0.51	0.02 (-0.36, 0.41); 0.90	-0.07 (-0.52, 0.38); 0.75	-0.05 (-0.50, 0.41); 0.83
ANAM M2S Mean RT	1380.69 (369.94); 30	1397.94 (440.89); 15	1363.44 (297.43); 15	-0.25, -34.50 (-317.57, 248.58); 0.80	0.11 (-0.28, 0.49); 0.58	0.09 (-0.35, 0.52); 0.69	0.06 (-0.37, 0.49); 0.78
ANAM SR2 Throughput	237.12 (34.96); 30	228.48 (46.28); 15	245.77 (15.16); 15	1.38, 17.29 (-9.25, 43.82); 0.19	-0.02 (-0.40, 0.37); 0.94	0.001 (-0.44, 0.44); 1.00	0.02 (-0.44, 0.47); 0.95
ANAM SR2 MeanRT	265.37 (92.09); 30	285.77 (128.30); 15	244.97 (14.62); 15	-1.22, -40.80 (-112.14, 30.55); 0.24	0 (-0.39, 0.39); 1.00	-0.02 (-0.46, 0.41); 0.91	-0.05 (-0.48, 0.38); 0.82
ANAM SRT Throughput	244.94 (19.54); 30	243.27 (21.17); 15	246.60 (18.36); 15	0.46, 3.40 (1.50, 18.17); 0.65	-0.06 (-0.45, 0.33); 0.75	-0.07 (-0.53, 0.38); 0.74	-0.06 (-0.52, 0.40); 0.79
RAVLT Trials 1 - 5 Total	50.57 (9.50); 30	52.20 (9.73); 15	48.93 (9.31); 15	-0.94, -3.27 (-10.39, 3.85); 0.36	-0.20 (-0.58, 0.18); 0.30	-0.16 (-0.61, 0.28); 0.46	-0.16 (-0.62, 0.29); 0.47
RAVLT Delayed Recognition Total	10.87 (3.75); 30	11.73 (3.33); 15	10.00 (4.05); 15	-1.28, -1.73 (-4.51, 1.05); 0.21	-0.28 (-0.66, 0.09); 0.13	-0.20 (-0.64, 0.24); 0.35	-0.20 (-0.65, 0.25); 0.37

TMT A Duration (in seconds)	29.3 (8.12); 30	31.60 (9.16); 15	27.00 (6.43); 15	-1.59, -4.60 (-10.55, 1.35); 0.12	-0.13 (-0.52, 0.25); 0.48	-0.12 (-0.55, 0.31); 0.57	-0.13 (-0.56, 0.31); 0.56
TMT B Duration (in seconds)	58.13 (16.63); 30	59.93 (18.29); 15	56.33 (15.20); 15	-0.59, -3.60 (-16.20, 9.00); 0.56	-0.07 (-0.46, 0.32); 0.72	-0.10 (-0.548, 0.35); 0.66	-0.10 (-0.56, 0.36); 0.66

Abbreviations: ANAM = Automated Neuropsychological Assessment Metrics; SRT = Simple Reaction Time; SR2 = Simple Reaction Time Repeat; CDS = Code Substitution — Learning; CDD = Code Substitution — Delayed; M2S = Matching to Sample; MTS = Mathematical Processing; TMT = Trail Making Test; RAVLT = Rey Auditory Verbal Learning Test

Note: Bonferroni-adjusted alpha level (0.05/11 tests) = 0.0045.

Table S13. Summary of Associations Between Self-Reported Psychological Health and Physical Symptoms Variables and Log-transformed GBEV

Measure	Full Sample M (SD); n	GBEVbelow (b) median group M (SD); n	GBEVabove (a) median group M (SD); n	$GBEV_a$ vs $GBEV_b$ t-statistic, difference in group means (95% CI); p-value	Unadjusted regression standardized beta, (95% CI); p-value	Adjusted regression standardized beta, (95% CI); p-value Covariates: age, combat exposure, blunt head trauma	Adjusted regression standardized beta, (95% CI); p-value Covariates: age, combat exposure, blunt head trauma, and PTSD symptom severity
Neurobehavioral Symptom Inventory Total	20.07 (12.09); 30	16.87 (9.43); 15	23.27(13.85); 15	1.48, 6.40 (-2.52, 15.32); 0.15	0.35 (-0.01, 0.71); 0.06	0.26 (-0.16, 0.68); 0.21	0.20 (-0.11, 0.51); 0.20
Buss Perry Total	74.53 (15.23); 30	73.33 (12.93); 15	75.73(17.61); 15	0.43, 2.40 (-9.20, 14.00); 0.67	0.16 (-0.23, 0.54); 0.41	0.20 (-0.26, 0.65); 0.34	0.15 (-0.26, 0.57); 0.45
Headache Impact Test–6 (HIT-6)	50.47 (9.22); 30	48.27 (8.61); 15	52.67 (9.57); 15	1.32, 4.40 (-2.41, 11.21); 0.20	0.39 (0.03, 0.74); 0.04	0.40 (-0.01, 0.81); 0.06	0.37 (-0.02, 0.77); 0.07
RAND36 – Physical Functioning	87.17 (10.72); 30	89.67 (9.72); 15	84.67(11.41); 15	-1.29, -5.00 (-12.94, 2.94); 0.21	-0.24 (-0.61, 0.14); 0.21	-0.03 (-0.44, 0.39); 0.90	0.004 (-0.40, 0.40); 0.99
RAND 36 – Role Limitations due to Physical Problems	65 (36.32); 30	71.67 (35.19); 15	58.33(37.40); 15	-1.00, -13.34 (-40.50, 13.83); 0.32	-0.26 (-0.64, 0.11); 0.16	-0.20 (-0.62, 0.23); 0.35	-0.17 (-0.59, 0.25); 0.40
RAND36 – Energy/Fatigue	40.67 (20.92); 30	41.58 (23.08); 15	39.75(19.29); 15	-0.24, -1.83 (-17.77, 14.10); 0.82	-0.19 (-0.57, 0.19); 0.31	-0.23 (-0.66, 0.21); 0.29	-0.18 (-0.56, 0.20); 0.34
RAND36 – Social Functioning	61.67 (22.25); 30	71.67 (17.97); 15	51.67(22.09); 15	-2.72, -20 (-35.09, -4.91); 0.011	-0.41 (-0.76, -0.06); 0.02	-0.36 (-0.75, 0.03); 0.07	-0.32 (-0.65, 0.02); 0.06
RAND36 – General Health	62.83 (17.60); 30	69.00 (16.06); 15	56.67(17.39); 15	-2.02, -12.33 (-24.86, 0.19); 0.05	-0.38 (-0.77, -0.02); 0.04	-0.45 (-0.85, -0.06); 0.03	-0.44 (-0.84, -0.04); 0.03

Note: Bonferroni-adjusted alpha level (0.05/8 tests) = 0.00625.

Table S14. Summary of Associations Between Blood Proteomics and Log-transformed GBEV

Measure	Full Sample M (SD); n	GBEVbelow (b) median group M (SD); n	GBEVabove (a) median group M (SD); n	$GBEV_a$ vs $GBEV_b$ t-statistic, difference in group means (95% CI); p-value	Unadjusted regression standardized beta, (95% CI); p-value	Adjusted regression standardized beta, (95% CI); p-value Covariates: age, combat exposure, blunt head trauma	Adjusted regression standardized beta, (95% CI); p-value Covariates: age, combat exposure, blunt head trauma, and PTSD symptom severity
phosphorylated Tau 181 (pTau181)	2.06 (1.70); 30	1.74 (0.60); 15	2.37 (2.32); 15	0.60, 0.11 (-0.28, 0.51); 0.55	0.13 (-0.26, 0.51); 0.50	0.14 (-0.33, 0.60); 0.55	0.13 (-0.34, 0.61); 0.57
Amyloid-β 40 (Aβ40)	160.87 (29.63); 30	157 (25.80); 15	164.73 (33.48); 15	0.57, 0.04 (-0.10, 0.18); 0.58	0.17 (-0.21, 0.55); 0.37	0.11 (-0.32, 0.54); 0.61	0.11 (-0.33, 0.56); 0.61
Amyloid-β 42 (Aβ42)	8.36 (1.26); 30	8.09 (0.98); 15	8.63 (1.48); 15	1.05, 0.06 (-0.06, 0.11); 0.30	0.30 (-0.06, 0.67); 0.10	0.10 (-0.27, 0.49); 0.56	0.11 (-0.28, 0.50); 0.57
Glial Fibrillary Acidic Protein (GFAP)	54.93 (15.12); 30	55.04 (16.23); 15	54.81 (14.49); 15	0.03, 0.003 (-0.20, 0.20); 0.98	-0.20 (-0.58, 0.18); 0.28	-0.20 (-0.60, 0.20); 0.32	-0.17 (-0.56, 0.22); 0.38
Neurofilament Light Chain (NfL)	6.72 (2.34); 30	6.22 (1.81); 15	7.23 (2.74); 15	1.04, 0.124 (-0.12, 0.37); 0.31	0.05 (-0.34, 0.44); 0.79	-0.04 (-0.49, 0.41); 0.84	-0.05 (-0.51, 0.42); 0.84
Tau N4	4.86 (3.86); 30	3.68 (1.85); 15	6.04 (4.95); 15	0.94, 0.26 (-0.32, 0.84); 0.36	0.31 (-0.06, 0.68); 0.10	0.39 (-0.03, 0.81); 0.07	0.41 (-0.003, 0.83); 0.05

Note: Bonferroni-adjusted alpha level (0.05/6 tests) = 0.0083.

Table S15. Summary of Associations Between 7 Tesla Resting-State Functional MRI and Log-transformed GBEV

Measure	Full Sample M (SD); n	GBEVbelow (b) median group M (SD); n	GBEVabove (a) median group M (SD); n	$GBEV_a$ vs $GBEV_b$ t-statistic, difference in group means (95% CI); p-value	Unadjusted regression standardized beta, (95% CI); p-value	Adjusted regression standardized beta, (95% CI); p-value Covariates: age, combat exposure, blunt head trauma	Adjusted regression standardized beta, (95% CI); p-value Covariates: age, combat exposure, blunt head trauma, and PTSD symptom severity
Default Mode	0.26 (0.10); 28	0.25 (0.10); 14	0.27 (0.10); 14	0.41, 0.02 (-0.06, 0.09); 0.69	0.13 (-0.27, 0.53); 0.52	0.16 (-0.30, 0.61); 0.48	0.13 (-0.34, 0.60); 0.56
Executive Control	0.36 (0.11); 28	0.39 (0.10); 14	0.32 (0.11); 14	-1.81, -0.07 (-0.15, 0.01); 0.08	-0.43 (-0.80, -0.07); 0.02	-0.50 (-0.92, -0.07); 0.03	-0.47 (-0.91, -0.04); 0.04
Salience	0.27 (0.09); 28	0.26 (0.08); 14	0.29 (0.10); 14	0.86, 0.03 (-0.04, 0.10); 0.40	0.02 (-0.40, 0.43); 0.90	0.23 (-0.19, 0.66); 0.26	0.18 (-0.23, 0.59); 0.37
Somatomotor	0.44 (0.16); 28	0.47 (0.18); 14	0.42 (0.14); 14	-0.87, -0.05 (-0.18, 0.07); 0.39	0.06 (-0.35, 0.46); 0.77	0.20 (-0.24, 0.65); 0.35	0.20 (-0.26, 0.66); 0.38

Note: Bonferroni-adjusted alpha level (0.05/4 tests) = 0.0125.

Table S16. Summary of Associations Between Connectome 3 Tesla MRI White Matter Integrity and Log-transformed GBEV

Measure	Full Sample M (SD); n	GBEVbelow (b) median group M(SD); n	GBEVabove (a) median group M (SD); n	$GBEV_a$ vs $GBEV_b$ t-statistic, difference in group means (95% CI); p-value	Unadjusted regression standardized beta, (95% CI); p-value	Adjusted regression standardized beta, (95% CI); p-value Covariates: age, combat exposure, blunt head trauma	Adjusted regression standardized beta, (95% CI); p-value Covariates: age, combat exposure, blunt head trauma, and PTSD symptom severity
Left CBD	0.61 (0.03); 30	0.61 (0.03); 15	0.61 (0.04); 15	0.01, 0.00 (-0.03, 0.03); 0.99	0.05 (-0.34, 0.43); 0.81	-0.02 (-0.47, 0.42); 0.92	-0.04 (-0.49, 0.41); 0.85
Right CBD	0.54 (0.04); 30	0.55 (0.04); 15	0.53 (0.04); 15	-1.27, -0.02(-0.05, 0.01); 0.22	-0.15 (-0.54, 0.23); 0.42	-0.194 (-0.65, 0.27); 0.39	-0.19 (-0.66, 0.28); 0.42
Left CBV	0.54 (0.04); 30	0.54 (0.04); 15	0.53 (0.04); 15	-0.70, -0.01 (-0.04, 0.02); 0.49	-0.01 (-0.40, 0.38); 0.95	-0.08 (-0.54, 0.37); 0.71	-0.08 (-0.55, 0.38); 0.72
Right CBV	0.53 (0.03); 30	0.53 (0.03); 15	0.52 (0.03); 15	-0.61, -0.007 (-0.03, 0.02); 0.55	0.02 (-0.37, 0.40); 0.94	-0.05 (-0.51, 0.41); 0.83	-0.05 (-0.53, 0.42); 0.83
Left ATR	0.5 (0.04); 30	0.51 (0.03); 15	0.5 (0.04); 15	-1.22, -0.02 (-0.05, 0.01); 0.23	-0.22 (-0.60, 0.16); 0.24	-0.32 (-0.75, 0.12); 0.15	-0.31 (-0.76, 0.14); 0.17
Right ATR	0.49 (0.04); 30	0.50 (0.03); 15	0.48 (0.04); 15	-1.60, -0.02 (-0.05, 0.01); 0.12	-0.29 (-0.66, 0.09); 0.13	-0.35 (-0.76, 0.07); 0.10	-0.35 (-0.78, 0.08); 0.10
Left UF	0.50 (0.04); 30	0.51 (0.03); 15	0.49 (0.04); 15	-1.00, -0.01 (-0.04, 0.02); 0.33	-0.21 (-0.59, 0.17); 0.27	-0.18 (-0.61, 0.26); 0.41	-0.17 (-0.62, 0.27); 0.43
Right UF	0.49 (0.04); 30	0.50 (0.03); 15	0.48 (0.04); 15	-1.27, -0.02 (-0.04, 0.01); 0.22	-0.24 (-0.62, 0.14); 0.20	-0.23 (-0.65, 0.19); 0.27	-0.22 (-0.65, 0.21); 0.29
Left ILF	0.53 (0.03); 30	0.54 (0.03); 15	0.53 (0.04); 15	-0.93, -0.01 (-0.04, 0.01); 0.36	-0.14 (-0.52, 0.24); 0.46	-0.16 (-0.61, 0.28); 0.46	-0.17 (-0.62, 0.29); 0.45
Right ILF	0.5 (0.03); 30	0.5 (0.03); 15	0.5 (0.04); 15	-0.17, -0.002 (-0.03, 0.02); 0.87	-0.15 (-0.53, 0.25); 0.45	-0.26 (-0.79, 0.17); 0.22	-0.27 (-0.71, 0.17); 0.22
Left CST	0.52 (0.03); 30	0.53 (0.02); 15	0.51 (0.04); 15	-1.48, -0.02 (-0.04, 0.01); 0.15	-0.31 (-0.68, 0.06); 0.10	-0.39 (-0.82, 0.03); 0.07	-0.42 (-0.84, 0.003); 0.05
Right CST	0.5 (0.03); 30	0.51 (0.02); 15	0.50 (0.04); 15	-0.94, -0.01 (-0.03, 0.01); 0.36	-0.26 (-0.64, 0.11); 0.16	-0.35 (-0.77, 0.07); 0.10	-0.37 (-0.79, 0.05); 0.08
Left SLF3	0.47 (0.04); 30	0.48 (0.03); 15	0.45 (0.04); 15	-1.76, -0.02 (-0.05, 0.004); 0.09	-0.26 (-0.64, 0.11); 0.16	-0.23 (-0.66, 0.21); 0.30	-0.24 (-0.68, 0.20); 0.27
Right SLF3	0.42 (0.03); 30	0.43 (0.03); 15	0.41 (0.04); 15	-0.96, -0.01 (-0.04, 0.01); 0.35	-0.25 (-0.62, 0.13); 0.18	-0.30 (-0.71, 0.10); 0.14	-0.32 (-0.73, 0.09); 0.12

Left EMC	0.52 (0.06); 30	0.54 (0.03); 15	0.51 (0.07); 15	-1.21, -0.03 (-0.07, 0.02); 0.24	-0.20 (-0.58, 0.18); 0.29	-0.12 (-0.56, 0.32); 0.57	-0.13 (-0.58, 0.32); 0.56
Right EMC	0.49 (0.03); 30	0.50 (0.03); 15	0.48 (0.04); 15	-1.65, -0.02 (-0.05, 0.01); 0.11	-0.23 (-0.61, 0.14); 0.22	-0.23 (-0.67, 0.21); 0.29	-0.23 (-0.67, 0.22); 0.31
CC Body C	0.56 (0.03); 30	0.56 (0.03); 15	0.56 (0.03); 15	0.04, 0.00 (-0.02, 0.02); 0.97	0.05 (-0.34, 0.44); 0.80	-0.14 (-0.57, 0.29); 0.50	-0.16 (-0.59, 0.27); 0.45
CC Genu	0.62 (0.03); 30	0.61 (0.03); 15	0.62 (0.03); 15	0.40, 0.004 (-0.02, 0.03); 0.70	0.10 (-0.29, 0.48); 0.61	0.06 (-0.38, 0.49); 0.78	0.07 (-0.38, 0.51); 0.75
CC Body P	0.58 (0.03); 30	0.58 (0.02); 15	0.58 (0.04); 15	-0.19, -0.003 (-0.03, 0.02); 0.85	0.02 (-0.37, 0.40); 0.94	-0.07 (-0.52, 0.37); 0.74	-0.08 (-0.53, 0.38); 0.74
CC Body PM	0.59 (0.03); 30	0.59 (0.03); 15	0.58 (0.03); 15	-0.65, -0.01 (-0.03, 0.02); 0.52	-0.06 (-0.44, 0.33); 0.77	-0.19 (-0.63, 0.25); 0.39	-0.19 (-0.64, 0.27); 0.41
CC Body PF	0.57 (0.03); 30	0.58 (0.02); 15	0.57 (0.03); 15	-0.45, -0.004 (-0.03, 0.02); 0.66	-0.14 (-0.52, 0.25); 0.47	-0.30 (-0.72, 0.12); 0.16	-0.31 (-0.74, 0.12); 0.15
CC splenium	0.64 (0.03); 30	0.64 (0.03); 15	0.64 (0.02); 15	0.66, 0.01 (-0.02, 0.03); 0.52	0.15 (-0.24, 0.53); 0.44	0.13 (-0.31, 0.58); 0.55	0.14 (-0.31, 0.60); 0.53
CC rostrum	0.63 (0.03); 30	0.62 (0.03); 15	0.63 (0.04); 15	0.62, 0.01 (-0.02, 0.03); 0.54	0.02 (-0.37, 0.41); 0.92	-0.06 (-0.48, 0.36); 0.77	-0.06 (-0.49, 0.37); 0.78
CC Body T	0.54 (0.03); 30	0.54 (0.03); 15	0.54 (0.04); 15	-0.31, -0.004 (-0.03, 0.02); 0.76	-0.05 (-0.44, 0.34); 0.80	-0.18 (-0.61, 0.26); 0.41	-0.18 (-0.63, 0.26); 0.41
MCP	0.47 (0.03); 30	0.48 (0.02); 15	0.47 (0.04); 15	-0.80, -0.01 (-0.03, 0.02); 0.43	-0.13 (-0.51, 0.26); 0.51	-0.15 (-0.58, 0.29); 0.50	-0.17 (-0.60, 0.26); 0.41

Abbreviations: ATR: anterior thalamic radiation; CC = corpus callosum; C = central section; P = parietal section; PF: prefrontal section; PM: premotor section; temporal; CBD: dorsal portion of cingulum bundle; CBV: ventral portion of the cingulum bundle; CC: corpus callosum; CST: corticospinal tract; EMC: extreme capsule; FAT: frontal aslant tract; ILF: inferior longitudinal fasciculus; ILF: middle longitudinal fasciculus; MCP = middle cerebellar peduncles; OR: optic radiation; SLF III: third branch of the superior longitudinal fasciculus; UF: uncinate fasciculus.

Note: Bonferroni-adjusted alpha level (0.05/25 tests) = 0.002.

Table S17. Summary of Associations Between Translocator Protein (TSPO) Measured by [^{11}C]PBR28 Positron Emission Tomography (PET) and Log-transformed GBEV

Measure	Full Sample M (SD); n	GBEVbelow (b) median group M (SD); n	GBEVabove (a) median group M (SD); n	$GBEV_a$ vs $GBEV_b$ t-statistic, difference in group means (95% CI); p-value	Unadjusted regression standardized beta, (95% CI); p-value	Adjusted regression standardized beta, (95% CI); p-value Covariates: age, combat exposure, blunt head trauma	Adjusted regression standardized beta, (95% CI); p-value Covariates: age, combat exposure, blunt head trauma, and PTSD symptom severity
Left medial orbitofrontal cortex	1.03 (0.03); 27	1.03 (0.02); 12	1.03 (0.03); 15	0.23, 1.03 (-0.02, 0.03); 0.82	0.006 (-0.41, 0.42); 0.98	0.10 (-0.41, 0.60); 0.69	0.09 (-0.44, 0.61); 0.74
Right medial orbitofrontal cortex	1.01 (0.03); 27	1.02 (0.03); 12	1.01 (0.03); 15	-0.51, 1.01 (-0.03, 0.02); 0.62	-0.13 (-0.54, 0.28); 0.51	-0.21 (-0.72, 0.30); 0.40	-0.26 (-0.75, 0.22); 0.27
Left rostral anterior cingulate cortex	0.99 (0.06); 27	0.98 (0.06); 12	0.99 (0.06); 15	0.64, 1.00 (-0.03, 0.06); 0.53	0.21 (-0.19, 0.62); 0.29	0.35 (-0.14, 0.84); 0.15	0.30 (-0.17, 0.76); 0.20
Right rostral anterior cingulate cortex	0.96 (0.08); 27	1 (0.07); 12	0.94 (0.07); 15	-2.12, 0.94 (-0.12, -0.00); 0.05	-0.43 (-0.80, -0.02); 0.03	-0.47 (-0.92, -0.02); 0.04	-0.50 (-0.95, -0.05); 0.03
Left rostral middle frontal gyrus	0.97 (0.03); 27	0.96 (0.02); 12	0.98 (0.03); 15	1.85, 0.98 (-0.00, 0.04); 0.08	0.20 (-0.21, 0.60; 0.32	0.22 (-0.23, 0.66); 0.32	0.20 (-0.25, 0.66); 0.37
Right rostral middle frontal gyrus	0.98 (0.03); 27	0.98 (0.03); 12	0.98 (0.03); 15	0.02, 0.98 (-0.02, 0.02); 0.99	0.06 (-0.36, 0.47); 0.79	-0.02 (-0.53, 0.50); 0.94	-0.05 (-0.57, 0.48); 0.86
Left superior frontal gyrus	1.03 (0.03); 27	1.03 (0.03); 12	1.03 (0.03); 15	0.18, 1.03 (-0.02, 0.02); 0.86	0.05 (-0.36, 0.46); 0.81	0.06 (-0.45, 0.56); 0.82	0.06 (-0.46, 0.58); 0.82
Right superior frontal gyrus	1.01 (0.02); 27	1.01 (0.02); 12	1.01 (0.03); 15	-0.60, 1.01 (-0.02, 0.01); 0.56	0.00 (-0.41, 0.41); 1.00	0.00 (-0.51, 0.51); 1.00	-0.03 (-0.55, 0.49); 0.90

Gray-white matter junction	0.99 (0.02); 27	0.99 (0.02); 12	1.00 (0.02); 15	1.55, 1.00 (0.01, 0.03); 0.13	0.25 (-0.15, 0.65); 0.21	0.10 (-0.37, 0.57); 0.66	0.12 (-0.36, 0.60); 0.61

Note: Bonferroni-adjusted alpha level (0.05/9 tests) = 0.006.

Table S18. Summary of Associations Between Tau Measured by [^{18}F]MK6240 Positron Emission Tomography (PET) and Log-transformed GBEV

Measure	Full Sample M (SD); n	GBEVbelow (b) median group M (SD); n	GBEVabove (a) median group M (SD); n	$GBEV_a$ vs $GBEV_b$ t-statistic, difference in group means (95% CI); p-value	Unadjusted regression standardized beta, (95% CI); p-value	Adjusted regression standardized beta, (95% CI); p-value Covariates: age, combat exposure, blunt head trauma	Adjusted regression standardized beta, (95% CI); p-value Covariates: age, combat exposure, blunt head trauma, and PTSD symptom severity
Left cerebellar cortex	1.19 (0.12); 28	1.19 (0.13); 13	1.19 (0.12); 15	-0.10, -0.01 (-0.10, 0.09); 0.92	-0.02 (-0.42, 0.39); 0.93	-0.14 (-0.53, 0.26); 0.48	-0.11 (-0.52, 0.29); 0.57
Right cerebellar cortex	1.23 (0.13); 28	1.23 (0.14); 13	1.23 (0.13); 15	0.10, 0.005 (-0.10, 0.11); 0.92	0.04 (-0.36, 0.44); 0.84	-0.13 (-0.49, 0.24); 0.48	-0.11 (-0.48, 0.27); 0.56
Left inferior parietal lobule	1.16 (0.1); 28	1.14 (0.08); 13	1.17 (0.11); 15	0.71, 0.03 (-0.05, 0.10); 0.49	0.14 (-0.26, 0.54); 0.48	0.15 (-0.29, 0.59); 0.49	0.16 (-0.29, 0.61); 0.47
Right inferior parietal lobule	1.22 (0.14); 28	1.18 (0.1); 13	1.25 (0.16); 15	1.32, 0.07 (-0.04, 0.17); 0.2	0.28 (-0.11, 0.67); 0.15	0.25 (-0.17, 0.67); 0.23	0.28 (-0.15, 0.70); 0.20
Left inferior temporal gyrus	1.31 (0.14); 28	1.29 (0.13); 13	1.33 (0.16); 15	0.74, 0.04 (-0.07, 0.15); 0.47	0.20 (-0.19, 0.60); 0.30	0.19 (-0.27, 0.64); 0.41	0.13 (-0.32, 0.58); 0.55
Right inferior temporal gyrus	1.36 (0.15); 28	1.34 (0.14); 13	1.37 (0.16); 15	0.66, 0.04 (-0.08, 0.15); 0.51	0.17 (-0.23, 0.57); 0.4	0.16 (-0.31, 0.63); 0.50	0.11 (-0.35, 0.57); 0.62
Left lateral occipital lobe	1.3 (0.14); 28	1.26 (0.11); 13	1.33 (0.15); 15	1.39, 0.069 (-0.033, 0.171); 0.176	0.324 (-0.06, 0.71); 0.093	0.25 (-0.15, 0.65); 0.21	0.26 (-0.15, 0.68); 0.20
Right lateral occipital lobe	1.33 (0.16); 28	1.3 (0.11); 13	1.35 (0.19); 15	0.99, 0.06 (-0.06, 0.17); 0.3	0.20 (-0.19, 0.60); 0.305	0.13 (-0.28, 0.55); 0.51	0.16 (-0.26, 0.58); 0.44

Left pars triangularis	1.14 (0.08); 28	1.12 (0.08); 13	1.16 (0.08); 15	1.41, 0.04 (-0.02, 0.10); 0.17	0.14 (-0.26, 0.54); 0.49	0.22 (-0.24, 0.68); 0.34	0.22 (-0.26, 0.70); 0.35
Right pars triangularis	1.21 (0.12); 28	1.17 (0.09); 13	1.25 (0.13); 15	1.76, 0.07 (-0.01, 0.16); 0.09	0.27 (-0.12, 0.66); 0.16	0.32 (-0.13, 0.77); 0.15	0.32 (-0.14, 0.79); 0.16
Left pericalcarine cortex	1.07 (0.08); 28	1.07 (0.08); 13	1.08 (0.09); 15	0.13, 0.004 (-0.06, 0.07); 0.90	0.08 (-0.32, 0.49); 0.68	0.05 (-0.40, 0.49); 0.84	0.07 (-0.38, 0.53); 0.74
Right pericalcarine cortex	1.05 (0.08); 28	1.04 (0.06); 13	1.07 (0.09); 15	0.86, 0.02 (-0.03, 0.08); 0.40	0.008 (-0.40, 0.41); 0.97	0.005 (-0.47, 0.48); 0.98	0.04 (-0.44, 0.52); 0.86
Left rostral middle frontal gyrus	1.16 (0.09); 28	1.14 (0.07); 13	1.17 (0.1); 15	0.90, 0.03 (-0.04, 0.098); 0.38	0.15 (-0.25, 0.55); 0.45	0.14 (-0.31, 0.58); 0.54	0.16 (-0.30, 0.62); 0.48
Right rostral middle frontal gyrus	1.21 (0.11); 28	1.19 (0.11); 13	1.22 (0.11); 15	0.61, 0.03 (-0.06, 0.11); 0.55	0.17 (-0.23, 0.57); 0.38	0.24 (-0.19, 0.67); 0.26	0.25 (-0.19, 0.70); 0.25
Left middle temporal gyrus	1.16 (0.08); 28	1.14 (0.06); 13	1.18 (0.09); 15	1.44, 0.04 (-0.02, 0.1); 0.16	0.26 (-0.13, 0.65); 0.18	0.21 (-0.21, 0.64); 0.31	0.20 (-0.24, 0.64); 0.36
Right middle temporal gyrus	1.24 (0.12); 28	1.22 (0.11); 13	1.27 (0.12); 15	1.16, 0.05 (-0.04, 0.14); 0.26	0.24 (-0.15, 0.63); 0.22	0.23 (-0.23, 0.68); 0.31	0.20 (-0.26, 0.66); 0.38

Note: Bonferroni-adjusted alpha level (0.05/16 tests) = 0.003.

Table S19. Summary of Associations Between Cortical Thickness and Log-transformed GBEV

Measure	Full Sample M (SD); n	GBEVbelow (b) median group M (SD); n	GBEVabove (a) median group M (SD); n	$GBEV_a$ vs $GBEV_b$ t-statistic, difference in group means (95% CI); p-value	Unadjusted regression standardized beta, (95% CI); p-value	Adjusted regression standardized beta, (95% CI); p-value Covariates: age, combat exposure, blunt head trauma	Adjusted regression standardized beta, (95% CI); p-value Covariates: age, combat exposure, blunt head trauma, and PTSD symptom severity
Left Banks of the Superior Temporal Sulcus	2476.87 (92.65); 30	2482.33 (64.62); 15	2471.40 (116.37); 15	-0.318, -10.93 (-82.23, 60.36); 0.75	0.11 (-0.27, 0.50); 0.55	0.19 (-0.27, 0.64); 0.41	0.16 (-0.29, 0.62); 0.47
Right Banks of the Superior Temporal Sulcus	2555.33 (115.96); 30	2537.80 (141.07); 15	2572.87 (85.42); 15	0.82, 35.07 (-53.01, 123.14); 0.42	0.11 (-0.28, 0.49); 0.58	0.12 (-0.33, 0.56); 0.59	0.14 (-0.31, 0.58); 0.53
Left Superior Frontal	2712.10 (104.25); 30	2722.47 (128.31); 15	2701.73 (76.26); 15	-0.54, -20.74 (-100.50, 59.03); 0.60	0.04 (-0.35, 0.42); 0.85	-0.06 (-0.48, 0.37); 0.80	-0.03 (-0.46, 0.39); 0.88
Right Superior Frontal	2685.57 (101.65); 30	2692.87 (118.39); 15	2678.27 (85.29); 15	-0.39, -14.60 (-92.12, 62.92); 0.70	0.09 (-0.30, 0.48); 0.63	0.04 (-0.41, 0.48); 0.87	0.070 (-0.36, 0.50); 0.75
Left Lateral Orbitofrontal	2679.07 (94.67); 30	2705.33 (66.13); 15	2652.80 (112.75); 15	-1.56, -52.53 (-122.42, 17.35); 0.13	-0.26 (-0.63, 0.12); 0.17	-0.11 (-0.54, 0.31); 0.59	-0.12 (-0.55, 0.32); 0.59
Right Lateral Orbitofrontal	2581.20 (96.15); 30	2588.40 (88.37); 15	2574.00 (105.98); 15	-0.40, -14.40 (-87.49, 58.69); 0.69	0.074 (-0.31, 0.46); 0.698	0.24 (-0.19, 0.68); 0.26	0.23 (-0.21, 0.68); 0.29

Left Rostral Middle Frontal	2361.37 (76.26); 30	2373.53 (73.43); 15	2349.2 (79.61); 15	-0.87, -24.33 (-81.63, 32.97); 0.39	-0.12 (-0.50, 0.27); 0.54	-0.25 (-0.67, 0.17); 0.24	-0.25 (-0.68, 0.18); 0.25
Right Rostral Middle Frontal	2300.80 (83.48); 30	2308.13 (61.82); 15	2293.47 (102.46); 15	-0.475, -14.67 (-78.58, 49.25); 0.64	0.05 (-0.34, 0.44); 0.80	-0.012 (-0.45, 0.43); 0.95	-0.02 (-0.47, 0.43); 0.92
Left Caudal Middle Frontal	2555.67 (131.21); 30	2583.00 (144.36); 15	2528.33 (114.98); 15	-1.15, -54.67 (-152.50, 43.16); 0.26	-0.14 (-0.53, 0.24); 0.45	-0.19 (-0.65, 0.26); 0.39	-0.15 (-0.55, 0.26); 0.47
Right Caudal Middle Frontal	2514.67 (125.06); 30	2534.60 (137.01); 15	2494.73 (113.02); 15	-0.87, -39.87 (-133.96, 54.22); 0.39	-0.02 (-0.41, 0.37); 0.91	-0.18 (-0.61, 0.26); 0.41	-0.15 (-0.57, 0.27); 0.48
Left Pars Triangularis	2504.57 (110.13); 30	2534.47 (128.74); 15	2474.67 (81.45); 15	-1.52, -59.80 (-141.04, 21.44); 0.14	-0.21 (-0.59, 0.17); 0.27	-0.21 (-0.66, 0.24); 0.35	-0.21 (-0.67, 0.25); 0.36
Right Pars Triangularis	2441.7 (74.51); 30	2449.33 (68.63); 15	2434.07 (81.64); 15	-0.55, -15.27 (-71.75, 41.22); 0.58	-0.10 (-0.49, 0.28); 0.59	-0.21 (-0.66, 0.25); 0.36	-0.20 (-0.66, 0.27); 0.39
Left Pars Opercularis	2599.93 (114.21); 30	2625.53 (123.75); 15	2574.33 (101.48); 15	-1.24, -51.20 (-135.99, 33.59); 0.23	-0.22 (-0.60, 0.15); 0.24	-0.17 (-0.61, 0.27); 0.428	-0.14 (-0.57, 0.28); 0.50
Right Pars Opercularis	2594.7 (105.66); 30	2587.47 (103.55); 15	2601.93 (110.85); 15	0.37, 14.47 (-65.78, 94.72); 0.72	-0.03 (-0.42, 0.36); 0.88	-0.15 (-0.59, 0.28); 0.48	-0.16 (-0.61, 0.29); 0.48
Left Pars Orbitalis	2619.33 (119.58); 30	2631.27 (110.46); 15	2607.4 (130.81); 15	-0.54, -23.87 (-114.54, 66.80); 0.59	-0.059 (-0.45, 0.33); 0.757	-0.16 (-0.57, 0.25); 0.43	-0.16 (-0.58, 0.26); 0.43
Right Pars Orbitalis	2628.50 (110.98); 30	2607.80 (126.02); 15	2649.2 (93.34); 15	1.02, 41.40 (-41.86, 124.66); 0.32	0.15 (-0.24, 0.53); 0.44	0.10 (-0.43, 0.44); 0.97	-0.002 (-0.45, 0.44); 0.99
Left Cuneus	1853.73 (147.95); 30	1866.07 (174.07); 15	1841.4 (121.31); 15	-0.45, -24.67 (-137.50, 88.16); 0.66	0.02 (-0.37, 0.41); 0.92	0.17 (-0.27, 0.60); 0.44	0.16 (-0.28, 0.61); 0.46
Right Cuneus	1856.63 (130.79); 30	1849.60 (141.27); 15	1863.67 (123.97); 15	0.29, 14.07 (-85.42, 113.55); 0.77	0.06 (-0.33, 0.44); 0.76	0.11 (-0.33, 0.55); 0.61	0.09 (-0.35, 0.53); 0.67
Left Pericalcarine	1634.60 (129.73); 30	1636.80 (123.39); 15	1632.4 (140.09); 15	-0.09, -4.40 (-103.21, 94.41); 0.93	0.21 (-0.17, 0.58); 0.28	0.28 (-0.15, 0.70); 0.20	0.28 (-0.15, 0.72); 0.19

Right Pericalcarine	1606.73 (146.09); 30	1638.87 (148.97); 15	1574.6 (140.73); 15	-1.22, -64.27 (-172.67, 44.14); 0.24	-0.27 (-0.64, 0.10); 0.15	-0.18 (-0.61, 0.25); 0.39	-0.17 (-0.61, 0.27); 0.43
Left Inferior Temporal	2745.23 (95.61); 30	2751.13 (111.61); 15	2739.33 (80.03); 15	-0.33, -11.80 (-84.78, 61.18); 0.74	-0.07 (-0.46, 0.31); 0.71	-0.07 (-0.53, 0.39); 0.75	-0.08 (-0.55, 0.39); 0.72
Right Inferior Temporal	2733.70 (92.43); 30	2747.53 (92.95); 15	2719.87 (92.99); 15	-0.815, -27.67 (-97.21, 41.87); 0.42	0.05 (-0.33, 0.44); 0.78	0.09 (-0.37, 0.55); 0.69	0.06 (-0.39, 0.51); 0.78
Left Middle Temporal	2836.00 (87.11); 30	2822.27 (108.88); 15	2849.73 (58.80); 15	0.86, 27.47 (-38.88, 93.81); 0.40	0.18 (-0.20, 0.56); 0.35	0.09 (-0.31, 0.49); 0.65	0.09 (-0.32, 0.50); 0.66
Right Middle Temporal	2756.80 (126.85); 30	2729.20 (147.53); 15	2784.4 (99.66); 15	1.20, 55.20 (-39.56, 149.96); 0.24	0.27 (-0.11, 0.64); 0.15	0.33 (-0.10, 0.76); 0.12	0.33 (-0.11, 0.77); 0.14
Left Supramarginal	2530.93 (104.72); 30	2522.40 (118.39); 15	2539.47 (92.43); 15	0.44, 17.07 (-62.59, 96.72); 0.66	0.22 (-0.16, 0.59); 0.25	0.27 (-0.17, 0.72); 0.22	0.28 (-0.18, 0.74); 0.22
Right Supramarginal	2530.83 (103.78); 30	2542.07 (87.67); 15	2519.6 (119.8); 15	-0.59, -22.47 (-101.31, 56.37); 0.56	0.07 (-0.32, 0.46); 0.71	0.17 (-0.26, 0.60); 0.42	0.18 (-0.26, 0.62); 0.41
Left Medial Orbitofrontal	2452.70 (92.24); 30	2446.20 (92.91); 15	2459.2 (94.35); 15	0.38, 13 (-57.04, 83.04); 0.71	0.23 (-0.14, 0.61); 0.22	0.30 (-0.14, 0.74); 0.17	0.31 (-0.14, 0.76); 0.16
Right Medial Orbitofrontal	2402.73 (122.62); 30	2383.33 (109.78); 15	2422.13 (135.22); 15	0.86, 38.80 (-53.50, 131.10); 0.40	0.32 (-0.05, 0.68); 0.09	0.50 (0.09, 0.90); 0.02	0.50 (0.09, 0.92); 0.02
Left Rostral Anterior Cingulate	2674.03 (163.64); 30	2609.67 (180.2); 15	2738.4 (118.82); 15	2.31,128.73 (13.77, 243.70); 0.03	0.59 (0.28, 0.90); 0.001	0.67 (0.33, 1.02); 0.0005	0.66 (0.31, 1.01); 0.001
Right Rostral Anterior Cingulate	2608.27 (187.65); 30	2581.27 (214.06); 15	2635.27 (159.85); 15	0.78, 54.00 (-87.82, 195.82); 0.44	0.38 (0.02, 0.74); 0.04	0.50 (0.09, 0.91); 0.02	0.50 (0.08, 0.92); 0.02
Left Frontal Pole	2676.00 (209.89); 30	2694.53 (136.21); 15	2657.47 (268.26); 15	-0.48, -37.07 (-198.72, 124.59); 0.64	-0.04 (-0.43, 0.35); 0.83	-0.13 (-0.59, 0.32); 0.55	-0.16 (-0.61, 0.29); 0.46
Right Frontal Pole	2645.47 (239.76); 30	2690.53 (212.71); 15	2600.4 (263.59); 15	-1.03, -90.13 (-269.64, 89.37); 0.312	-0.03 (-0.42, 0.36); 0.87	0.02 (-0.42, 0.46); 0.92	0.002 (-0.44, 0.44); 0.99

Left Insula	2907.83 (135.22); 30	2910.40 (150.51); 15	2905.27 (123.31); 15	-0.10, -5.13 (-108.22, 97.96); 0.92	0.02 (-0.37, 0.41); 0.91	0.17 (-0.26, 0.60); 0.43	0.18 (-0.27, 0.62); 0.42
Right Insula	2930.90 (156.89); 30	2908.87 (186.28); 15	2952.93 (123.49); 15	0.76, 44.10 (-74.95, 163.10); 0.45	0.33 (-0.04, 0.69); 0.08	0.45 (0.03, 0.87); 0.04	0.45 (0.02, 0.88); 0.04

Note: Bonferroni-adjusted alpha level (0.05/34 tests) = 0.00147.

Table S20. Summary of Significant Associations Between Measures and Log-transformed GBEV

Domain	Variable	Unadjusted regression standardized beta, (95% CI); p-value	Adjusted regression standardized beta, (95% CI); p-value Covariates: age, combat exposure, blunt head trauma	Adjusted regression standardized beta, (95% CI); p-value Covariates: age, combat exposure, blunt head trauma, and PTSD symptom severity
Self-Report Measures of Psychological Health and Physical Symptoms	General Health – RAND36	-0.38 (-0.74, -0.02); 0.04	-0.45 (-0.85, -0.06); 0.03	-0.44 (-0.84, -0.04); 0.03
	Social Functioning – RAND36	-0.41 (-0.76, -0.06); 0.02	-0.36 (-0.75, 0.03); 0.07	-0.32 (-0.65, 0.02); 0.06
	HIT-6	0.39 (0.03, 0.74); 0.04	0.40 (-0.009, 0.81); 0.06	0.37 (-0.02, 0.77); 0.07
Cortical Thickness	Left rACC thickness	0.59 (0.28, 0.90); 0.001	0.67 (0.33, 1.02); 0.0005	0.66 (0.31, 1.01); 0.001
	Right rACC thickness	0.38 (0.02, 0.74); 0.04	0.50 (0.10, 0.91); 0.02	0.50 (0.08, 0.92); 0.02
	Right insula thickness	0.33 (-0.04, 0.69); 0.08	0.45 (0.03, 0.87); 0.04	0.45 (0.02, 0.88); 0.04
	Right medial orbitofrontal cortical thickness	0.32 (-0.05, 0.68); 0.09	0.50 (0.09, 0.90); 0.02	0.50 (0.09, 0.92); 0.02
TSPO	Right rACC TSPO levels	-0.43 (-0.80, -0.05); 0.03	-0.47 (-0.92, -0.02); 0.04	-0.50 (-0.95, -0.05); 0.03
Resting State Functional MRI	Executive Control Network	-0.43 (-0.80, -0.07); 0.02	-0.50 (-0.92, -0.07); 0.03	-0.47 (-0.91, -0.04); 0.04

Abbreviations: HIT-6 = Headache Impact Test–6; rACC = rostral anterior cingulate cortex; TSPO = Translocator Protein; MRI = magnetic resonance imaging.

Note: Bonferroni-adjusted alpha levels were generated for each measurement domain (0.05/the number of variables in the subdomain). The adjusted alpha level for the psychological health and physical symptoms domain was 0.00625 (0.05/8 tests). The adjusted alpha level for the resting state functional MRI domain was 0.0125 (0.05/4 tests). The adjusted alpha level for the TSPO PET domain was 0.0055 (0.05/ 9 tests). The adjusted alpha level for the cortical thickness domain was 0.00147 (0.05/34 tests). We adjusted for PTSD symptoms using PCL-5 score as a continuous variable.

Table S21. Summary of Association Between Cortical Thickness Derived from T1 MEMPRAGE Data Acquired during PET-MRI scan and Log-transformed GBEV

Measure	Full Sample M (SD); N	GBEVbelow (b) median group M (SD); n	GBEVabove (a) median group M (SD); n	$GBEV_a$ vs $GBEV_b$ t-statistic, difference in group means (95% CI); p-value	Unadjusted regression standardized beta, (95% CI); p-value	Adjusted regression standardized beta, (95% CI); p-value
Left Rostral Anterior Cingulate Cortex	2509.03 (112.35); 30	2479.67 (107); 15	2538.4 (113.36); 15	1.46, 58.73 (-23.73, 141.19); 0.156	0.42 (0.07, 0.78); 0.019	0.58 (0.19, 0.96); 0.005

Table S22. Summary of Associations Between PCL-5 Score and Log-transformed GBEV

Variable	Unadjusted regression standardized beta, (95% CI); p-value	Adjusted regression standardized beta, (95% CI); p-value Covariates: age, combat exposure, time in service	Adjusted regression standardized beta, (95% CI); p-value Covariates: age, combat exposure, blunt head trauma
PCL-5 continuous	0.19 (-0.20, 0.57); 0.33	0.19 (-0.28, 0.66); 0.42	0.09 (-0.35, 0.54); 0.67

Abbreviation: PCL-5 = PTSD Checklist for DSM-5.

Note: PCL-5 scores can range from 0 to 80, with higher scores reflecting more severe symptoms.

Table S23. Comparisons Between Blast Exposure Groups on Weight, Radiochemistry Measures, TSPO Genotype, and SUV of regions used for SUV normalization

	Parameter	**p-value**
*[^{11}C]PBR28 TSPO scan**		
Weight (via independent sample t-test)	t = -0.35	0.73
TSPO Genotype (via Fisher's exact test)	N/A	0.34
[^{11}C]PBR28 injected dose (via independent sample t-test)	t = 1.21	0.25
[^{11}C]PBR28 molar activity (via independent sample t-test)	t = 0.42	0.68
Whole brain SUV** (dependent variable in linear regression)		
Group (independent variable in linear regression)	beta = -0.06	0.18
Genotype (independent variable in linear regression)	beta = -0.24	< 0.001
*[^{18}F]MK6240 tau scan****		
Weight (via independent sample t-test)	t = -0.79	0.44
[^{18}F]MK6240 injected dose (via independent sample t-test)	t = -1.06	0.30
[^{18}F]MK6240 molar activity (via independent sample t-test)	t = -1.18	0.25
Isthmus cingulate cortex SUV (via independent sample t-test)	t = -1.39	0.18

* Three participants were excluded for [^{11}C]PBR28 TSPO PET analyses due to TSPO genotype conferring low affinity binding.
** This analysis is controlling for TSPO genotype and excluding one participant whose TSPO genotype is undetermined.
*** Two participants that did not have a [^{18}F]MK6240 tau scan were not included.
Abbreviations: TSPO=translocator protein, SUV=standardized uptake value

Table S24. Demographics and Exposures for $GBEV_a$ and $GBEV_b$ groups

Characteristic	$GBEV_b$ (n=15)	$GBEV_a$ (n=15)	P Value
Age – yr	36.1 ± 4.2	38.0 ± 3.5	0.19
Sex: Male – no.	15	15	---
Race: White– no.	15	15	
Ethnicity: Non-Hispanic – no.	13	14	
Education – yr.	17.1 ± 2.2	16.6 ± 1.9	0.55
Years in Service	16.4 ± 5.0	18.0 ± 3.7	0.33
Military Branch – no.	11 Army 2 Navy 2 Air Force 0 Marines	9 Army 2 Navy 2 Air Force 2 Marines	0.91
Rank – no. Officer Warrant Officer Enlisted	 1 2 12	 0 2 13	0.60
CES Score	31.7 ± 4.6	36.1 ± 4.4	0.01
Combat Exposure (CES) – no. Moderate Moderate-Heavy Heavy	 2 6 7	 0 4 11	0.23
Surrounded by Enemy – no. 0 times 1-2 times 3-12 times 13-25 times 26+ times	 1 1 5 3 5	 0 0 1 0 14	0.002
Blows to the Head (BISQ) – no. Low High	 6 9	 3 12	0.43
Cumulative Blast Exposure (GBEV)	3,141,510 (387,860 to 9,424,695)	26,506,000 (9,763,085 to 363,812,869)	---
Most Recent Blast Exposure – no. <1 year 1 year 2 years	 12 1 2	 14 1 0	---

Plus–minus values are means ± SD. The Generalized Blast Exposure Value (GBEV) (32) is reported as median (range). Blows to the head "high" = number of participants with more blows to the head than they could remember; "low" = number of participants who could recall a finite number of blows to the head (range of blows to the head: 1-13),assessed by the Brain Injury Screening Questionnaire (BISQ) (33). Abbreviations: CES = Combat Exposure Scale (34); $GBEV_a$ = GBEV above the median; $GBEV_b$ = GBEV below the median.

SI References.

1. P. Green, "Green's Medical Symptom Validity Test (MSVT) for Microsoft Windows: User's Manual.". (Green's Publishing, Edmonton, Canada, 2004).
2. R. D. Vanderploeg *et al.*, Screening for postdeployment conditions: development and cross-validation of an embedded validity scale in the neurobehavioral symptom inventory. *J Head Trauma Rehabil* **29**, 1-10 (2014).
3. A. S. Vincent, T. Roebuck-Spencer, K. Gilliland, R. Schlegel, Automated Neuropsychological Assessment Metrics (v4) Traumatic Brain Injury Battery: military normative data. *Mil Med* **177**, 256-269 (2012).
4. S. Vermeent, M. Spaltman, G. van Elswijk, J. B. Miller, B. Schmand, Philips IntelliSpace Cognition digital test battery: Equivalence and measurement invariance compared to traditional analog test versions. *Clin Neuropsychol* **36**, 2278-2299 (2022).
5. R. M. Braga, K. R. A. Van Dijk, J. R. Polimeni, M. C. Eldaief, R. L. Buckner, Parallel distributed networks resolved at high resolution reveal close juxtaposition of distinct regions. *J Neurophysiol* **121**, 1513-1534 (2019).
6. K. Setsompop *et al.*, Blipped-controlled aliasing in parallel imaging for simultaneous multislice echo planar imaging with reduced g-factor penalty. *Magn Reson Med* **67**, 1210-1224 (2012).
7. B. Fischl, FreeSurfer. *NeuroImage* **62**, 774-781 (2012).
8. M. E. Raichle, The restless brain. *Brain Connect* **1**, 3-12 (2011).
9. S. Y. Huang *et al.*, High-gradient diffusion MRI reveals distinct estimates of axon diameter index within different white matter tracts in the in vivo human brain. *Brain Struct Funct* **225**, 1277-1291 (2020).
10. J. Jovicich *et al.*, Reliability in multi-site structural MRI studies: effects of gradient non-linearity correction on phantom and human data. *NeuroImage* **30**, 436-443 (2006).
11. J. L. Andersson, S. Skare, J. Ashburner, How to correct susceptibility distortions in spin-echo echo-planar images: application to diffusion tensor imaging. *NeuroImage* **20**, 870-888 (2003).
12. J. L. R. Andersson, S. N. Sotiropoulos, An integrated approach to correction for off-resonance effects and subject movement in diffusion MR imaging. *NeuroImage* **125**, 1063-1078 (2016).
13. J. L. R. Andersson, M. S. Graham, E. Zsoldos, S. N. Sotiropoulos, Incorporating outlier detection and replacement into a non-parametric framework for movement and distortion correction of diffusion MR images. *NeuroImage* **141**, 556-572 (2016).
14. T. E. Behrens *et al.*, Characterization and propagation of uncertainty in diffusion-weighted MR imaging. *Magn Reson Med* **50**, 1077-1088 (2003).
15. C. Maffei *et al.*, Using diffusion MRI data acquired with ultra-high gradient strength to improve tractography in routine-quality data. *NeuroImage* **245**, 118706 (2021).
16. A. Yendiki *et al.*, Automated probabilistic reconstruction of white-matter pathways in health and disease using an atlas of the underlying anatomy. *Front Neuroinform* **5**, 23 (2011).
17. A. J. W. van der Kouwe, T. Benner, D. H. Salat, B. Fischl, Brain morphometry with multiecho MPRAGE. *NeuroImage* **40**, 559-569 (2008).
18. A. M. Dale, B. Fischl, M. I. Sereno, Cortical surface-based analysis. I. Segmentation and surface reconstruction. *NeuroImage* **9**, 179-194 (1999).
19. B. Fischl *et al.*, Automatically parcellating the human cerebral cortex. *Cereb Cortex* **14**, 11-22 (2004).
20. B. Fischl *et al.*, Whole brain segmentation: automated labeling of neuroanatomical structures in the human brain. *Neuron* **33**, 341-355 (2002).

21. M. D. Tisdall *et al.*, Prospective motion correction with volumetric navigators (vNavs) reduces the bias and variance in brain morphometry induced by subject motion. *NeuroImage* **127**, 11-22 (2016).
22. N. R. Zurcher *et al.*, [(11)C]PBR28 MR-PET imaging reveals lower regional brain expression of translocator protein (TSPO) in young adult males with autism spectrum disorder. *Mol Psychiatry* **26**, 1659-1669 (2021).
23. D. R. Owen *et al.*, An 18-kDa translocator protein (TSPO) polymorphism explains differences in binding affinity of the PET radioligand PBR28. *J Cereb Blood Flow Metab* **32**, 1-5 (2012).
24. D. Izquierdo-Garcia *et al.*, An SPM8-based approach for attenuation correction combining segmentation and nonrigid template formation: application to simultaneous PET/MR brain imaging. *J Nucl Med* **55**, 1825-1830 (2014).
25. C. N. Ladefoged *et al.*, A multi-centre evaluation of eleven clinically feasible brain PET/MRI attenuation correction techniques using a large cohort of patients. *NeuroImage* **147**, 346-359 (2017).
26. S. B. Shively *et al.*, Characterisation of interface astroglial scarring in the human brain after blast exposure: a post-mortem case series. *Lancet Neurol* **15**, 944-953 (2016).
27. D. Benjamini, D. S. Priemer, D. P. Perl, D. L. Brody, P. J. Basser, Mapping astrogliosis in the individual human brain using multidimensional MRI. *Brain* **146**, 1212-1226 (2023).
28. P. A. Harris *et al.*, Research electronic data capture (REDCap)--a metadata-driven methodology and workflow process for providing translational research informatics support. *J Biomed Inform* **42**, 377-381 (2009).
29. C. M. W. Tax, M. Bastiani, J. Veraart, E. Garyfallidis, M. Okan Irfanoglu, What's new and what's next in diffusion MRI preprocessing. *NeuroImage* **249**, 118830 (2022).
30. R. S. Desikan *et al.*, An automated labeling system for subdividing the human cerebral cortex on MRI scans into gyral based regions of interest. *NeuroImage* **31**, 968-980 (2006).
31. B. L. Edlow *et al.*, Long-Term Effects of Repeated Blast Exposure in United States Special Operations Forces Personnel: A Pilot Study Protocol. *J Neurotrauma* **39**, 1391-1407 (2022).
32. L. C. M. Modica, M. J. Egnoto, J. K. Statz, W. Carr, S. T. Ahlers, Development of a Blast Exposure Estimator from a Department of Defense-Wide Survey Study on Military Service Members. *J Neurotrauma* **38**, 1654-1661 (2021).
33. K. Dams-O'Connor *et al.*, Screening for traumatic brain injury: findings and public health implications. *J Head Trauma Rehabil* **29**, 479-489 (2014).
34. T. M. Keane *et al.*, Clinical evaluation of a measure to assess combat exposure. *Psychological Assessment* **1**, 53-55 (1989).